1951

Isomeric metastable states in medium and heavy weight nuclei.

Francis, Arthur Eugene

Massachusetts Institute of Technology

ISOMERIC METASTABLE STATES IN MEDIUM AND HEAVY WEIGHT NUCLEI

A. E. FRANCIS

1951

ISOMERIC METASTABLE STATES IN MEDIUM AND HEAVY WEIGHT NUCLEI

by

Author Eugene Francis

M.E. Stevens Institute of Technology
(1942)

M.S. Massachusetts Institute of Technology
(1948)

Submitted in Partial Fulfillment of the
Requirements for the Degree of
Master of Science in Physics

at the

Massachusetts Institute of Technology
(1951)

Signature of Author _____

Department of Physics, July 1, 1951

Certified by _____

Thesis Supervisor

_____

Chairman, Departmental Committee on Graduate Students

ISOMERIC METASTABLE STATES IN MEDIUM AND HEAVY WEIGHT NUCLEI

by

Arthur Eugene Francis

Submitted for the Degree of Master of Science in the Department of Physics on July 17, 1951

ABSTRACT

The 48.6-minute metastable state was formed in Cd^{111} by the inelastic scattering of monoergic fast neutrons on natural cadmium. The neutrons were obtained by bombarding a Li^7 target with monoergic protons from the Rockefeller generator at M.I.T. The presence of excited levels in Cd^{111} at energies of 0.720 ± 0.020 Mev and 1.150 ± 0.020 Mev was detected. The threshold for the formation of the metastable state was determined as 0.400 ± 0.25 Mev. Therefore, either the 0.420-Mev level or the 0.396-Mev, 48.6-minute, metastable level was excited directly. Either an $l = 3$ or an $l = 4$ neutron combines with Cd^{111} to form the compound nucleus which emits an $l = 0$ neutron. If the 48.6-minute metastable state was excited directly, and that is almost certain, its angular momentum is either 11/2 or 9/2; the angular momentum of the 5×10^{-5}-second metastable state is either 5/2 or 3/2; the parities of the two metastable states are opposite to the parity of the ground state if the incoming neutron has $l = 3$; and the parities are the same as the parity of the ground state if the incoming neutron has $l = 4$.

$l = 8$.

TABLE OF CONTENTS

TABLE OF CONTENTS

LIST OF FIGURES

List of Figures

LIST OF TABLES

I. INTRODUCTION

The determination of the energy, angular momentum, and parity of excited levels in nuclei is an important step in obtaining information concerning nuclear structure.

These characteristics of excited levels can be obtained from observations of transitions between specific excited states and between excited states and the ground state in nuclei. Such transitions often occur after a nuclear reaction leaves the nucleus in an excited state. However, these excited states usually have very short lifetimes.

Nuclear isomers are nuclei having the same number of protons and neutrons, but differing in their stability or mode of radioactive decay. The simplest case of nuclear isomerism occurs when one of the isomers is a stable nucleus in its ground state and the other is an excited state of the same nucleus. When an excited state exists for a measurable length of time, it is called a metastable state. Metastable states differ from other excited states only because of their slower rate of decay.

In 1921, Otto Hahn, the German radiochemist, produced evidence that uranium Z and uranium X_2, both naturally occurring nuclides, were isotopic and isobaric, but had different radioactive decay rates. For several years, this remained as the only substantiated case of nuclear isomerism. In 1935, it was discovered that the bombardment of $_{35}Br^{79}$ by slow neutrons produced two isomers of Br^{80} with different half-lives. Since that time, many examples of nuclear isomerism have

1. Introduction

The determination of the exterior, algebraic monodromy, and order
[illegible] of rational functions is an objective
[illegible] dynamical systems.

These [illegible] of analytic [illegible] can be obtained from
observations of [illegible] [illegible] analytic models and [illegible]
analytic [illegible] that [illegible] is analytic. Most [illegible] [illegible]
[illegible] a [illegible] analytic [illegible] [illegible] is an analytic [illegible]
[illegible]. [illegible] analytic [illegible] [illegible] [illegible].

[illegible] [illegible] are modeled [illegible] [illegible] of [illegible]
and machines, [illegible] [illegible] [illegible] [illegible] of [illegible]
[illegible]. The [illegible] [illegible] of [illegible] [illegible] [illegible] [illegible] of the
[illegible] is a [illegible] [illegible] [illegible] [illegible] [illegible] it as
analytic [illegible] of [illegible] [illegible]. [illegible] an [illegible] [illegible] [illegible]
a [illegible] [illegible] [illegible] it [illegible] is [illegible] a [illegible] [illegible]. [illegible]
[illegible] [illegible] [illegible] [illegible] [illegible] [illegible] [illegible] [illegible]
[illegible] [illegible] of [illegible].

In 1921, [illegible] [illegible] [illegible] [illegible], [illegible] [illegible]
[illegible] [illegible] [illegible] $\mathbb{C}_\infty$ [illegible] [illegible] [illegible] [illegible],
[illegible] [illegible] not [illegible], but [illegible] [illegible] [illegible] [illegible]
[illegible] [illegible], [illegible] [illegible] is [illegible] [illegible] [illegible] of
[illegible] [illegible]. In 1978, it was discovered that [illegible] [illegible] of
z^{29} is also [illegible] [illegible] [illegible] of z^{29} [illegible] [illegible]
[illegible]. [illegible] [illegible] [illegible], [illegible] [illegible] of [illegible] [illegible]
[illegible].

been discovered. As measurement techniques improve, more radioactive nuclides are being reclassified as isomeric.

Weizsacker provided the first theoretical explanation for the existence of isomers. He showed that by assigning to the excited state an angular momentum which differs from the ground state by 3 to 5 units and an energy of a few hundred kilovolts or less, a half-life is predicted for transition to the ground state by gamma-ray emission which is long enough to be observable.

Isomeric metastable states result from interactions between high-energy X-rays or electrons and stable nuclei and from the nuclear excitation which accompanies the inelastic scattering of alpha particles, deuterons, protons, or fast neutrons. Inelastic scattering of neutrons is a convenient method of producing excited states in nuclei, but cross sections for such reactions are small, and large inherent backgrounds are encountered. However, if the lifetime of the excited state is long enough, the transition to a lower state may be observed after the beam of exciting particles has been removed and after competing reactions have died away. Therefore, the existence of metastable states provides a method of studying energy levels in nuclei. Comparison of the experimentally obtained cross section for the formation of the metastable state in a particular nucleus with the theoretical cross section for the formation of the same state often facilitates estimating the spin and parity of the metastable state and of other excited levels in that nucleus.

The half-lives of the various known isomers range from fractions of seconds to years, and there is no qualitative difference between an excited state with a very short life and one with a long life. Isomers have not been found in nuclei having mass numbers below 39. The characteristics (half-life, excitation energy, decay scheme, conversion ratios, etc.) of isomers of stable nuclei may be found in various tabulations of nuclear data, such as Seaborg and Pearlman (S1), Sullivan (S2), and Nuclear Data NBS 499 (N1). Segre and Helmholtz (S3) have assembled complete data on all but the most recently discovered isomers. A careful survey of their tables is required when selecting a particular isomer for experimental investigation. The experimenter must be sure that there are no other radiations arising from accompanying nuclear reactions which seriously interfere with the detection of the decay of the metastable state.

When the activity of a metastable state is plotted against the energy of the exciting radium, changes in the slope of the curve occur as new excited levels of the stable nucleus are reached. The excitation curve changes shape because additional higher excited levels in the target nucleus become available for decay to the metastable state as the excitation energy increases, and an increase in the cross section for formation of the metastable state is produced. Wiedenbeck (W1, W2, W3, W4) has obtained such excitation curves which indicate excited levels that decay to the metastable state for Au^{197}, Rh^{103}, Cd^{111}, and both isotopes of Ag. Wiedenbeck (W4) also reports excitation of

the threshold level alone in Au^{197} by bombardment with fast neutrons of broad energy distribution, and he states that the neutron threshold is the same as the one obtained in his X-ray work.

Waldman and Wiedenbeck (W5), using X-rays as an exciting medium, have reported a series of excited levels which decay to the metastable state in In^{115}. Goldhaver, Hill, and Szilard (G1) have confirmed the existence of a metastable state in In^{115} by inelastic scattering of fast neutrons. The metastable state in In^{115} has also been excited by Barnes and Aradine (B1) with protons and by Lark-Horovitz, Risser, and Smith (L1) with high-energy alpha particles. Both Cohen (C1) and Taschek (T1) have obtained excitation curves for In^{115}, bombarded by fast neutrons which indicate only the threshold level.

The quanta employed in the foregoing work involving the use of X-rays were obtained by bombarding thick targets with monoergic electrons. Consequently, the X-rays were continuous in energy distribution. Prior to 1950, no experimenters had used monoergic heavy particles to determine excited levels by inelastic scattering for an appreciable range of energies above the metastable state. The use of either quanta or heavy particles with a substantial energy distribution results in only slight changes in the slope of the excitation curve at energy levels. Therefore, the exact location and sometimes even the existence of excited levels is subject to question. Kbel (K1), using monoergic fast neutrons

as a source of excitation, located several energy levels in Au^{197} and In^{115}. The changes in slope of the monoergic neutron excitation curves at energy levels are pronounced enough to inspire considerable confidence. All the levels determined by Ebel appear to be slightly lower than the corresponding levels previously determined by quantum excitation. This thesis describes the use of Ebel's technique in investigating the metastable state and higher energy excited states in Cd^{111}.

II. THEORY

Half-Lives of Excited States

Segre and Helmholtz (S3) have presented a detailed review of Weizsacker's theory of nuclear isomerism. Another good survey of various theories of nuclear isomerism is given by Hole (H1). Such theoretical quantitative explanations for the measurable lifetimes of metastable states are complicated by the dearth of detailed information about the nucleus. Consequently, many different methods for calculating half-lives of metastable states have been suggested, each justified by different assumptions concerning the nature of the nucleus. Bethe (B2), Hebb and Uhlenbeck (H2), Lowen (L2), and others have determined formulas for predicting the probability of transition from an excited level to a lower level by gamma-ray emission. Moon (M1) gives a graph, based on a simplification of Lowen's formula, of decay constants vs. gamma-ray energy for various multipole values of radiation. This curve is a convenient method of estimating either the half-life, the multipole order, of the transition energy of a particular gamma-ray transition when two of three parameters are known quantities.

Selection Rules for Gamma-Ray Transitions

The general theory regarding gamma-ray emission (selection rules, decay constants, spin, parity, etc.) includes transitions from

II. THEORY

[illegible] of Isomeric States

[illegible] and [illegible] ([illegible]) have presented a detailed review of Weizsäcker's theory of nuclear isomerism. Another good survey of various theories of nuclear isomerism is given by [illegible] ([illegible]). The theoretical quantitative explanations for the measurable lifetimes of metastable states are complicated by the degree of detailed information about the nucleus. Consequently, many different methods for calculating half-lives of metastable states have been suggested, each justified by different assumptions concerning the nature of the nucleus. [illegible] ([illegible]), [illegible] and [illegible] ([illegible]), [illegible] ([illegible]), and others have developed formulas for predicting the probability of transition from an excited level to a lower level by gamma-ray emission. [illegible] ([illegible]) gives a graph, based on a simplification of [illegible]'s formula, of decay constants vs. gamma-ray energy for various multipole orders of radiation. This curve is a convenient method of estimating either the half-life, the multipole order, or the transition energy of a particular gamma-ray transition when two of these parameters are known quantities.

Selection Rules for Gamma-Ray Transitions

The general theory regarding gamma-ray emission (selection rules, decay constants, spin, parity, etc.) includes transitions from

the metastable state. The quantum theory of radiation utilizes the classical concept of a radiation source as an oscillating electric or magnetic moment. The radiations are classified as 2^{ℓ} electric or magnetic dipole, quadrupole, octupole, etc., where ℓ is the angular momentum carried away by the gamma ray in units of $\hbar$. Since the vector angular momentum of the system is conserved in all nuclear reactions, the emission of a gamma ray by a nucleus changes its angular momentum in accordance with the multipole order of the radiation. The absolute difference in angular momentum between two states in a nucleus determines the lowest allowed multipole order radiation that can occur in a transition between the states ($\ell_{min} = /I/-/I'/$). Higher order multipole radiations up to $\ell_{max} = /I/+/I'/$ are possible. However, the probability per unit time of radiation occurring decreases rapidly as the multipole order increases, so the lowest allowed multipole order is usually the only one which contributes appreciably to the transition, except that an electric $2^{\ell+1}$-pole may be a serious competitor to a magnetic 2^{ℓ}-pole.

The parity of a state is said to be odd (-) or even (+) depending on whether a reversal of sign of all the coordinates of the system does or does not reverse the sign of the wave function describing the state. Parity, like angular momentum, is conserved in a nuclear reaction. The parity of even electric and odd magnetic multipoles is taken as even (+) and the parity of odd electric and even magnetic multipoles is taken as odd (-). Therefore, if two states have the same

parity, a transition between them involves only even electric or odd magnetic multipole orders, and if two states have opposite parity, the transition between them involves only odd electric and even magnetic multipole orders.

The importance of the angular momentum and parity selection rules is manifested in the long lifetime of a metastable state.

Internal Conversion

A nucleus in an excited state may spontaneously change to a state of lower energy by emitting a gamma ray of energy equal to the energy difference between the two states or by giving this increment of energy to an atomic electron in one of its own shells. This "internal conversion" electron is ejected from the atom with a kinetic energy equal to the corresponding quantum energy less the atomic binding energy of the electron and the energy of recoil. Originally it was thought that the energy of the nuclear transition was first emitted as a gamma ray, which then ejected a photo-electron from the atom. Taylor and Mott (T1) showed that internal conversion is actually a primary rather than secondary process and is due to the direct interaction of the nucleus with its own electrons. Therefore, the probability per unit time of decay of an excited state may be the sum of the probabilities of the competing gamma-ray emission and internal conversion instead of the probability of gamma-ray emission only. The probability of internal conversion may be even greater than that

of gamma-ray emission. The ejection of the conversion electron causes a vacancy in the electronic structure of the atom, and therefore, it is followed immediately by the emission of characteristic X-rays of the element in question.

The conversion coefficient is the ratio of the rate of emission of conversion electrons to the rate of emission of gamma rays. The total rate of electron emission is the sum of the rates for the various atomic shells (K, L, etc.). The conversion coefficient is complicated to calculate theoretically and difficult to determine experimentally. Dancoff and Morrison (D1) have obtained an expression for K-electron conversion coefficients which treats the ejected electron nonrelativistically and have also obtained an approximate relativistic expression which neglects electron binding energy. Another source of K-shell internal conversion coefficients is an extensive table which has been privately distributed by Rose (R1). The ratio of the K-shell to the L-shell conversion coefficients is relatively easy to determine experimentally because it is only necessary to compare the intensity of two lines in the same electron spectrum. Comparison of experimental and theoretical K/L ratios affords a means of determining whether a gamma-ray transition is an electric or magnetic multipole.

Axel and Dancoff (A1) have found good agreement between the experimentally determined lifetimes of about 50 isomers and the theoretical lifetimes predicted by the Wiezsacker hypothesis and corrected for internal conversion.

Neutron Excitation of Metastable Levels

Excitation of a metastable state in a nucleus by bombarding the nucleus with fast neutrons is a special case of inelastic scattering of fast neutrons. The process is shown diagrammatically in Figure 1. Bombardment by neutrons with less energy than the energy of the first excited state of the target nucleus, E_1, results in simple elastic scattering, and the nucleus is left in its ground state. If the neutron energy is higher than E_1, the compound nucleus can decay to E_1 or to the ground state of the target nucleus. The lowest neutron energy capable of leaving the target nucleus in its first excited state is the energy of that state. The metastable state generally is only a few hundred kilovolts above the ground state and will be one of the first levels to be excited. The selection rules which prevent the rapid decay of a metastable state may also prevent its ready excitation from the ground state directly. Since both selection rules and energy requirements must be satisfied in nuclear reactions, it may be necessary to excite a higher energy level which will decay by gamma-ray emission to the metastable state. Figure 1 shows the direct and indirect methods of producing state E_1 (assumed metastable) in a hypothetical nucleus. The method which actually produces the metastable state depends on the specific selection rules which operate.

The cross section for exciting a metastable state is the product of the cross section, σ_c, for exciting the compound nucleus and the probability, W_g, that it will decay to the metastable state.

Summary and Introduction

Investigations of a synchronous motor in a medium of variable
resistance with constant reactance E. A general case of variable
resistance and reactance. The relation to power characteristic
in figure 1. Investigations by oscillograph which have recently given the ex-
tension of the linear operating characteristic $\frac{E^2}{2r}$ possible
to slightly exceed maximum power. The limit is that at which
operation. At the maximum it is higher than $\frac{E^2}{2r}$. The maximum
can occur for $\frac{E^2}{2r}$ but the power exceeds at this maximum. The
limiting operating condition is limited by the maximum possible in the
system operating with it. The characteristic
which possibility is also a function of this relation. The
other possibility is that of the stable limits in the condition. The maximum
point which is not at the stable limits is the condition. The maximum
point which is not at the stable limits is the condition. The maximum
point which is not at the stable limits is

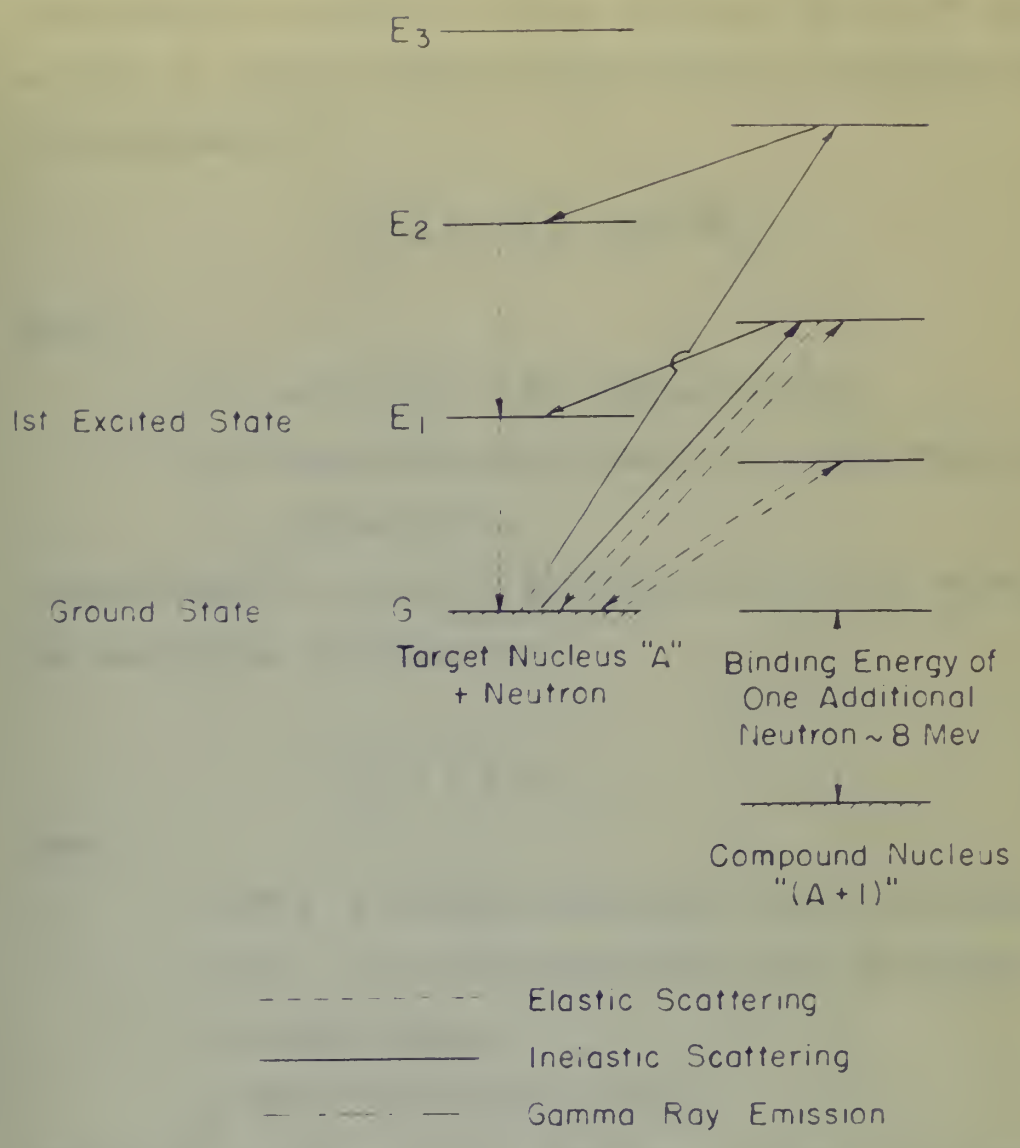

Figure 1

SCHEMATIC DIAGRAM OF NEUTRON SCATTERING

Blatt and Weisskopf (B3) have derived an expression for the cross section for the formation of the compound nucleus by neutron bombardment as a function of neutron energy and the orbital angular momentum, ℓ, of the incoming neutron relative to the target nucleus. The expression is:

$$\sigma_c(\ell) = (2\ell + 1)\pi\lambda^2 T_\ell \quad ,$$

where

λ = wave length of the incident neutron,

T_ℓ = transmission coefficient for a neutron through the nuclear surface.

Assuming there is no potential for neutrons outside the target nucleus, the transmission coefficient is:

$$T_\ell = 4\left(\frac{x}{X}\right)v_\ell \quad ,$$

where

$x = kR$; k = neutron wave number outside the nucleus,

$X = KR$; K = neutron wave number inside the nucleus,

R = nuclear radius,

v_ℓ = factor depending on x and ℓ.

Methods for computing K and v are given by Blatt and Weisskopf.

The probability for decay of the compound nucleus to a given excited state of the target nucleus may be determined by utilizing the

Blatt and Weisskopf (23) have derived an expression for the cross section for the formation of the compound nucleus by neutron bombardment as a function of neutron energy and the orbital angular momentum, l, of the incident neutron relative to the target nucleus. The expression is

$$\sigma_c(l) = (2l+1)\pi\chi_\lambda^2 T^l \quad .$$

where

χ = wave length of the incident neutron,

T^l = transmission coefficient for a neutron through the nuclear surface.

Assuming there is no interaction between the incoming neutron, the transmission coefficient may be approximated by

$$T^l = \rho \left(\frac{x}{2}\right)^{2l} \quad .$$

where

$x = kR$; k = neutron wave number inside the nucleus,

R = nuclear radius,

λ^l = Legendre polynomial in x and l.

The probability for capture of the compound nucleus to a given excited state of the target nucleus may be determined by multiplying the probabilities for combined E and λ as given by Blatt and Weisskopf.

reciprocity theorem

$$\frac{\sigma(A \rightarrow B)}{(\lambda_A)^2} = \frac{\sigma(B \rightarrow A)}{(\lambda_B)^2} ,$$

which relates the cross sections for transitions in both directions between two states. Considering neutron emission as the only method of decay, the probability of the compound nuclei decaying to a state having energy E_1 above the ground state of the target nucleus compared to the n other states having energies E_i above the ground state is:

$$W_1 = \frac{(E - E_1)\sigma_c(E_1, l)}{\sum_{i=1}^{i=n} (E - E_i)\sigma_c(E_i, l)} ,$$

where

$\sigma_c(E_i, l)$ = cross section for formation of the compound nucleus from level i ,

E = energy available for decay of the compound nucleus to the ground state of the target nucleus.

The cross section for the formation of the metastable state cannot be accurately computed unless the cross sections for the formation of the compound nucleus from all possible levels in the target nucleus are known. The calculation outlined above applies specifically to the case where the metastable state is formed only by direct decay from the compound nucleus. In many cases the compound nucleus will decay to an intermediate excited state, which then decays to the metastable state. When this condition

$$\frac{\alpha(\chi \to \beta)}{\alpha(\beta \to \chi)} = \frac{\chi^{\beta}_{\chi}}{\chi^{\chi}_{\beta}} \quad (\chi^{\beta})$$

which relates the cross sections for interactions to both directions between two states. Considerable caution should be used in using detailed balance, for example, the assumption implied comparing it a state at energy, the probability of the backward implied comparing it a state having energy E^{β} above the energy state of the initial neutron

to the a ground state, initial nucleus B^{β} minus the ground state for

$$\frac{\alpha^{\beta} = \dfrac{\sum_{E=0}^{E=E^{\beta}} (2 - \delta^{\beta}) \alpha(\beta^{\beta}, \gamma)}{(2 - \delta^{\beta}) \alpha(\beta^{\beta}, \gamma)}}{}$$

where

$\alpha(\beta^{\beta}, \gamma)$ = cross section for formation of the compound nucleus

nucleus into level β.

δ = energy variable for energy of the compound nucleus in the ground state of the target nucleus.

The cross section for the formation of the antimatter state cannot be conveniently computed unless the above conditions for the formation of the compound nucleus meet all necessary levels in the target nucleus are known. The calculation multiplied above applies directly to the case where the compound nucleus is formed only by capture when the compound nucleus. Is only cause the compound nucleus will decay to an indistinguishable particle state, which then decays to the metastable state. When this condition

exists, appropriate corrections, involving probabilities of gamma-ray emission, must be applied to the above calculation.

Neutron Versus Photon Excitation of Metastable States

During the process of inelastic scattering, a target nucleus may absorb from any incident neutron the energy required to raise itself to an excited state, providing the neutron possesses kinetic energy equal to or greater than the energy of the particular excited state. However, for the case of photons, production of an excited state in a target nucleus involves line absorption of only photons of the same energy as that of the excited state.

When a metastable state is produced in a nucleus, the exciting medium must carry in the angular momentum required to change the spin of the nucleus from that of the ground state to that of the metastable state. Direct production of a metastable state by quantum excitation is very improbable because the same selection rules which insure the long lifetime of a metastable state also prevent the nucleus from absorbing radiation corresponding to a transition from the ground state to the metastable state. Under such a limitation, metastable states, produced by practical intensities of photon bombardment, must be formed in two steps. A highly excited state of the nucleus is produced, which then decays by gamma-ray transitions. A fraction of these decays is to the metastable state.

Neutrons have a higher probability than quanta of carrying into the target nucleus the 3 or 4 units of angular momentum usually

required to excite the metastable state directly from the ground state. Kbel (K1), using monoergic fast neutrons as bombarding particles, was able to excite the metastable state directly from the ground state in Au^{197}, but not in In^{115}. Of course, neutrons have a greater probability of carrying only one or two units of angular momentum into a target nucleus and, therefore, may also excite those higher energy levels which are excited directly from the ground state by photon bombardment.

III. EXPERIMENTAL EQUIPMENT

Source of Neutrons

The $Li^7(p,n)Be^7$ reaction, which gives a relatively high yield of nearly monoergic neutrons, was used as a source of fast neutrons for this experiment. If neutrons of known and constant energy are to be obtained from this reaction, the energy of the protons must be accurately known and must remain constant throughout individual excitation runs. Protons with the required characteristics were obtained from the M.I.T. Rockefeller electrostatic generator.

The $Li^7(p,n)$ reaction is endoergic, having a Q value of - 1.63 Mev. At its threshold, 1.88 Mev, it supplies 0.029-Mev neutrons in the forward direction.

The target was prepared by evaporating metallic lithium onto a tantalum backing. To insure a uniform target thickness and to prevent boiling off of the lithium during generator operation, the tantalum backing was located eccentric to both the lithium furnace and the proton beam and was continuously rotated during target preparation or proton bombardment. The vacuum, which is maintained in the accelerator tube and deflection chamber, prevents the lithium from being oxidized. Target thicknesses were determined by Taschek and Hemmendinger's (T2) method of assuming the thickness in Kev to equal the energy increment between the neutron threshold and the

first (geometrical) peak of the yield curve for zero degrees. The tantalum backing stops all the protons, but does not react with neutrons.

Rockefeller Generator

The unanalyzed beam of charged particles consists of protons and diatomic and triatomic hydrogen ions. The accelerating tube is kept under vacuum, so that the ions suffer very few collisions and are nearly monoergic. The voltage across the terminals of the generator determines the energy of the beam. After passing down the accelerating tube, the proton beam is bent through 90 degrees by an analyzing magnetic field. The beam is focused at the top of the tube by a lens of adjustable voltage. Its cross section is defined at the bottom of the tube by two pairs of crossed adjustable slits. The details of the principle, operation, and use of the machine have been well covered in the literature (J1, W6, P1).

A nuclear-resonance method is used for controlling the field of the analyzing magnet. This allows fine control and accurate measurement of the energy of the proton beam. The frequency of the nuclear resonance is measured and is related to the energy of the protons in the beam by the expression (Schoenfeld and Duborg (S4), Hadden (H3)):

$$E = kf^2,$$

where

E = proton energy,

f = frequency of nuclear resonance.

Lovington (L3) gives the total uncertainty in the proton energy as ± 5 Kev.

The neutron energy may be calculated using the measured value of proton energy and the laws of conservation of mass-energy and momentum. A table of neutron energies corresponding to various proton energies has been calculated in this manner by Willard (W6) and was used by the author for this investigation.

Measurement of Neutron Yield

The yield of neutrons was measured with a long counter similar in design to that of Hanson and McKibben (H4). This counter is shown in Figure 2. The cadmium shield prevents neutrons of very low energy (multiply scattered from the floor, walls, etc.) from entering the paraffin, and, therefore, most of the neutrons which reach the central BF_3 counter have only thermal energy. Experiments have proved that these characteristics of construction, together with the correct combination of physical dimensions, make a counter of this type equally sensitive to all neutrons with energies between 0.5 and 2.5 Mev (H4, W6). The counter used during this investigation decreases in relative sensitivity for neutrons with energies below 0.5 Mev, as shown in Figure 3 (W6).

The associated electronic equipment consisted of:

(a) Regulated high-voltage supply (M.I.T. Servomechanisms Laboratory, Electronic Nuclear Instrumentation Project).

(b) Model 100 preamplifier.

[illegible] (2) given the local connectivity in the moving images as
2 D time.

The question should not be calculated using the computed
values of stereo models and the lines of correspondence in previous
and successive. A lack of motions accurate correspondence in previous
motion sequence has been calculated in this chapter to multiple lag
and was taken by the motion for this investigation.

Improvement of Image Flow

The photo of sequence was calculated with a long exposure sim-
ilar to photos in terms of lenses and lighting (sol). This monitor is
shown in Figure 3. The evaluation selected commonly examples of many low
quality (particularly contrasted from the first, until, about five notable
the procedure, and, alternatively, some of the conditions which cannot the
problems 37) provided there only changed results. Improvements have proved
that these discrepancies of consideration, together with the overall
application of digital dimensions make a problem of this type equally
possible to all problems with accuracy [illegible] and 3 and [illegible].
[illegible]. The computer used digital this investigation displacement in relative
satisfactorily for analysis with recognize below 0.3 pixel. We shown in
Figure 3 (36).

The associated discussion mathematical consistent of:

(a) Magnified high-quality images in L.I.R. Correspondence
[illegible]; Illustrated Black-and Instrumentation Problem).

(b) [illegible] [illegible].

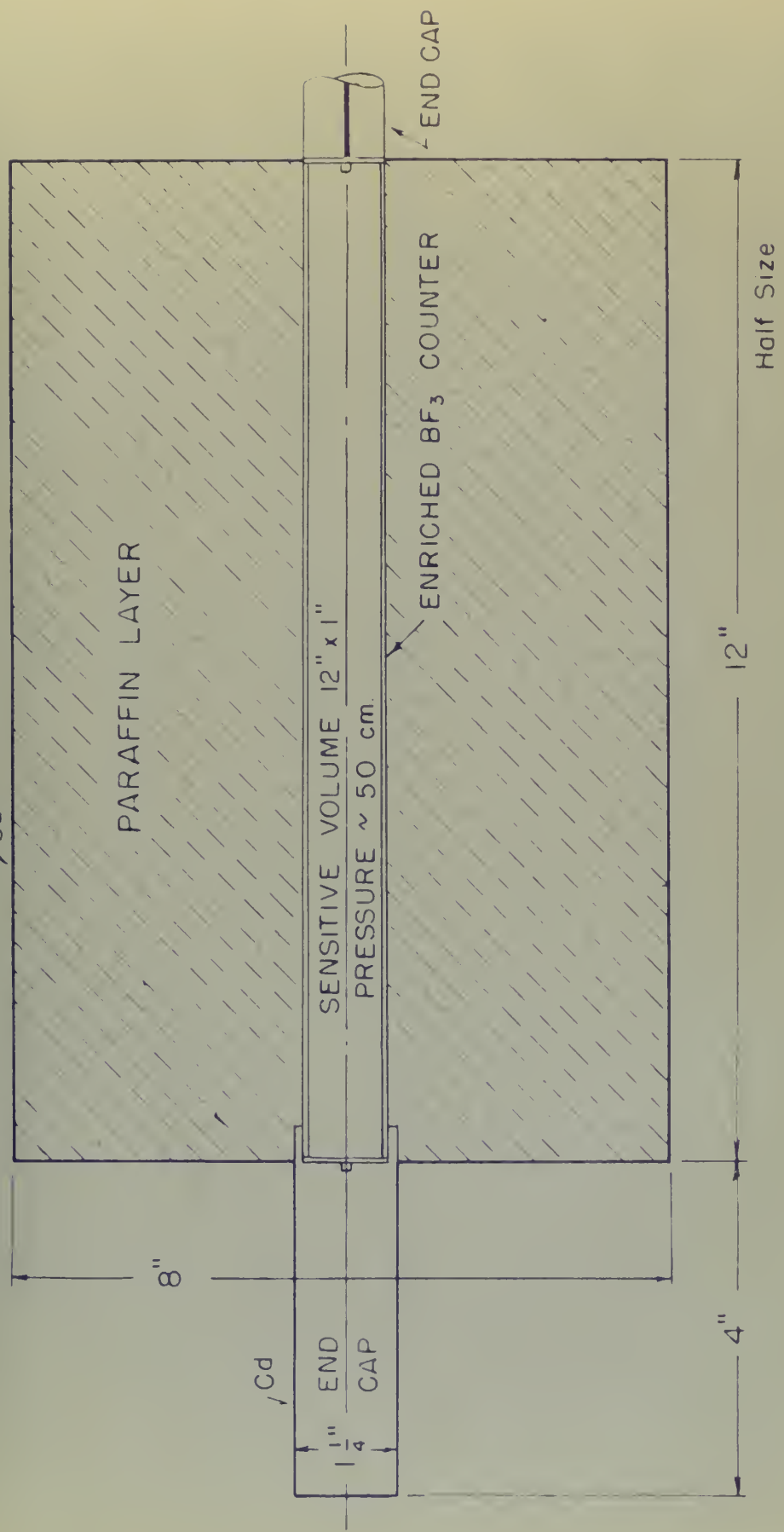

Figure 2

LONG COUNTER

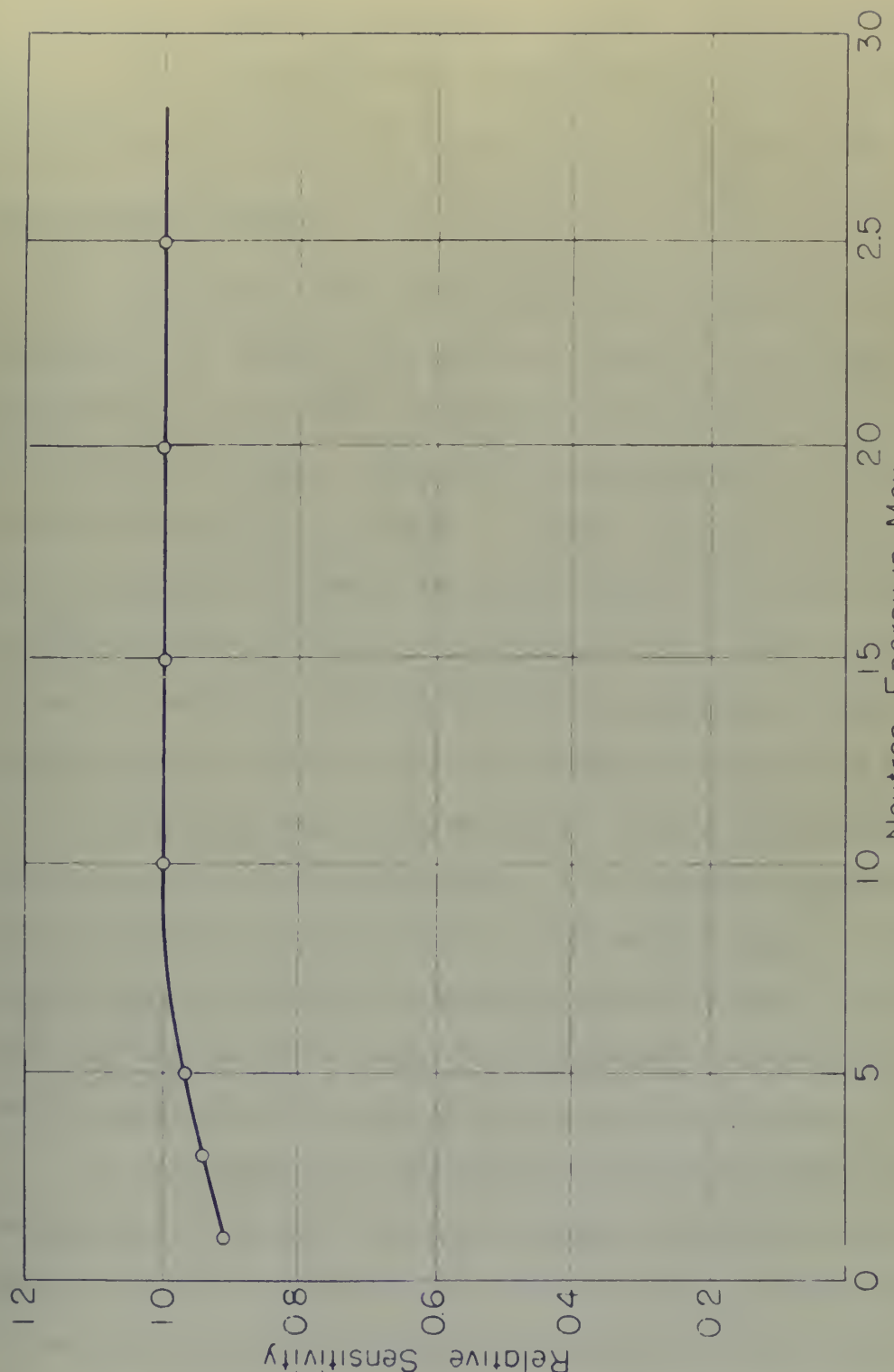

Figure 3

RESPONSE OF THE LONG COUNTER TO MONOENERGETIC NEUTRONS

(c) Model 100 amplifier.

(d) Model 105 Atomic Instrument Company decade scaler.

Items (b) and (c) are described in detail by Elmore and Sands (E2).

Scintillation Counter

The decay of the metastable state was detected by means of a scintillation counter. The counter consisted of an RCA type 5819 photomultiplier tube with an anthracene crystal cemented to its window with Canada balsam. The crystal was approximately 1 1/2 inches in diameter and 5/16 inch thick. In order to increase the light reflection inside the crystal, its exposed sides were covered with 0.00025-inch aluminum foil. A 0.04-inch mu metal shield, for the purpose of reducing stray magnetic fields, surrounded the sides of the tube and the crystal. The entire counter was encased in a 3-inch lead shield, which reduced the background due to stray radiation. The lead shield was also light-tight. A brass slider, extending into the lead shield, permitted rapid and convenient changing of experimental samples. The slider contained a circular cavity, for receiving 3-cm. diameter foils or disks, which positioned the sample in line with the axis of the tube and about 3 mm. from the crystal.

The output of the phototube is extremely sensitive, even to very small fluctuations in input voltage. Therefore, if comparable results are to be reproduced over a period of time, voltage stability is necessary throughout the electronic setup associated with the scintillation counter. Sola constant-voltage transformers were used as

(c) Model 100 multiplexer.

(d) Model 107 Remote Diagnostic Processor Remote Console.

Items (b) and (c) are described in Section 3F Models 100.

Configuration Overview

The layout of this configuration might be thought of as those of a multiplexing operation. The computer connected at the 103 type 2103 interface sends data out on multiplexer output channel to the selected line at 1.2/3 inches per minute and 9/16 inch steps. It appears to interpret the right hand direction inside the computer, its output control which controls the 0.0009-inch clearance first. A U.S.-made or model 100/01, for the purposes of indicating start sequence direction, determines the value of the byte and the crystal. The write monitor was accessed in a 3-inch load which, which reduced the beginning line to start position. The load which was also light-right. A three slider, automatic data the load which, processing begin and accumulated changing at sequential control. The slider contained a terminal unit, for terminating 3-cm. direction line up right, which positioned the sample in time with the ratio of the byte and above 3 on, then the sequence.

The output of the photograph is automatic sometimes, when be very small dimensions in input variable. Sometimes, it manipulate above to be processed over a period of time, written alphabetic is necessary through the electronic motor connected with the motion operation. Data accept-multiple transformers were found in

sources of power for all electronic units, and a special voltage stabilizer was inserted between the high-voltage supply and the phototube input.

The power for the phototube was supplied by a regulated high-voltage supply of the type described in the previous section. The phototube signal was fed through a cathode-follower preamplifier into a Model 100 amplifier (M2). The output from the amplifier was fed into a Model 210 (scale-of-32) single-channel differential discriminator which had been altered in themanner described in Appendix A.

The reproducibility of results given by this equipment was established by counting the decay of radioactive standards at frequent intervals during the investigation.

Platinum-Screen Counter

A platinum-screen gamma-ray counter, which is currently used by the Radioactivity Center of the M.I.T. Physics Department for determining absolute disintegration rates, was employed to obtain the absolute rate of emission of gamma rays by a sample of Hg^{203}. The counter is similar to the platinum-screen counter investigated by Peacock (P2) during his determination of gamma-ray counter efficiencies. The standardized Hg^{203} sample was needed for estimating the efficiency of the scintillation counter.

IV. INVESTIGATION OF Cd^{111}

Historical Background of the Excitation of Metastable Cd^{111}

Mattuch, the Austrian physicist, has postulated two rules regarding the existence of metastable states:

(a) Isomerism does not occur in nuclei having an even number of protons and an even number of neutrons.

(b) Isomerism occurs only in nuclei which have ground-state spins of 1/2 or 9/2 or greater.

Pb^{204}, an even-even nucleus, is usually reported as having a 68-minute metastable state (not definitely established as isomeric) and appears to violate rule (a). Au^{197}, having a ground-state spin of 3/2 and a 7.5-second metastable state, violates rule (b). However, such rules should not be expected to be without exception, and they at least suggest possible isomeric nuclei for a given mass number.

Cd^{111}, with a ground-state spin of 1/2, conforms with both of Mattuch's rules. Therefore, it was not surprising that Wiedenbeck (W7), in 1944, reported the existence of a 48.6-minute metastable state in Cd^{111}. Wiedenbeck erroneously determined this energy to be 0.195 Mev above the ground state. Hole (H1), in 1947, determined spectrographically that the energy of the metastable state was 0.381 Mev above the ground state and that it decayes by gamma emission to a level 0.235 Mev above the ground state, which then decayed to the ground state by gamma emission. The currently accepted values for these levels, 0.396 Mev and 0.247 Mev, were determined by Helmholtz, Hayward, and McGinnis (H5) with

11. Synthesis of DE_{123}

Preliminary Investigation of the Identification of Isopentenyldiphosphate (DE_{123})

Purpose: The following discussion, when presented and duly considered, will establish the validity of the following:

(a) Isopentenyl alcohol can be used to convert Dmapp to Grpp.

(b) Isopentenyl alcohol can be used to convert Grpp to Frpp.

Grpp yields at least 1/3 as much Frpp as Dmapp.

DE_{123}, or some-what similar, is commonly considered to produce a Dmapp-Grpp-Frpp pattern (and therefore metabolite) when incubated in Isopentenyl and dimethyl in ethanolic buffer (1). DE_{123} treated a pentane-ether mix of 3/5 and a 2,3-pentanone metabolite pattern, ethanol-free mix (3). However, many more chromatograms had to be examined to get this pattern, and those at least showed significant inhibition of the a Dmapp spot.

DE_{123} yields a pentane-ether mix of 3/5 resulting with both of the metabolite patterns. Therefore, it was considered that Isopentenyl (IP), in DE_{123}, accounted for a DMC-isomerase activity in the DE_{123} that alters the Dmapp spot. Since (IP) in DE_{123} derivatized dimethylallyl-diphosphate (DMAPP), it was considered that DMAPP could be converted to a Grpp spot by the DE_{123} that alters the Grpp spot. The experiment was designed to test the presence of DMAPP in DE_{123} by incubating DE_{123} with Dmapp and Isopentenyl alcohol. The experiment was designed to test the presence of DMAPP in DE_{123} by incubating DE_{123} with Dmapp and Isopentenyl alcohol. The experiment was designed to test the presence of DMAPP in DE_{123} by incubating DE_{123} with Dmapp and Isopentenyl alcohol.

a magnetic lens spectrograph. Goldhaber and Muelhause (G2), by observing the (n,γ) reaction in Cd^{110}, have confirmed that the 48.6-minute metastable state exists in Cd^{111}. Deutsch (D2, D3) subsequently determined that the 0.247-Mev excited level decayed with a half-life of 5×10^{-8} second, and this level has been reclassified as a second metastable state in Cd^{111}. Therefore, this isotope is unique because it is the only stable nucleus currently known to have more than one metastable state.

Energy Levels in Cd^{111}

Figure 4 is an energy level diagram for Cd^{111}. It contains all of the currently published information (W1) about the decay of the excited states of the nucleus and about the decay of neighboring isotopes to Cd^{111} by beta emission and K-capture. The presence of the four highest excited levels was indicated by Wiedenbeck's (W7) excitation curves for the 48.6-minute metastable state. He obtained curves for both X-ray and electron bombardment of Cd^{111}. The threshold energy observed by Wiedenbeck for production of the metastable state was 1.25 Mev for both types of excitation.

The theoretical half-lives against decay by gamma-ray emission of several different multipole orders for both metastable states of Cd^{111} have been calculated by the author using various formulas based on the Wiezsacker hypothesis. The half-lives obtained by these calculations, both uncorrected and corrected for internal conversion, are presented in Table I.

a magnetic Zeeman experiment. Applications and theorems (QE), for ex-
ecuted the (E,F) ensemble to Cd_{112}, have contributed that the $^1S_0$-
ciently antisymmetric cusps appears in Cd_{111}. Insofar (E, CD) subsequently
determined that the 0.247-Ion ensemble Zeeman decayed with a half-life of
$8 \approx 10^{-6}$ seconds, and this level has been provisionally in a bombed pho-
ninety photon in Cd_{111}. Elsewhere, this function is simple because it
is the only stable nuclear monotonically known to have only spin one
metastable state.

Proton levels in Cd_{111}

Figure 1 is an energy level diagram for Cd_{111}. By analogy
all of the isotopically published information (E3) about the decay of the
excited states of the neutron and count the decay of neighboring iso-
topes to Cd_{111} By this notation and F-capture. The presence of the
four highest excited levels was indicated by Richardson's [E7] work-
ing before the $^1S_0$-second nuclear state. We obtained excess
for both X-ray and electron measurements of Cd_{111}. The discovery energy
observed by Richardson the positions of the metastable state was 1.35
via the beta types of emissions.

The theoretical half-life implies almost zero Gamow-Teller mix-
ing of nuclear singlet multipole orders for both metastable states
of Cd_{113} have been calculated by the nuclear shell model Eigenstates
based on the Nilsson hypothesis. The half-life obtained by these
calculations, both consistent and corrected for internal conversion,
are presented in Table I.

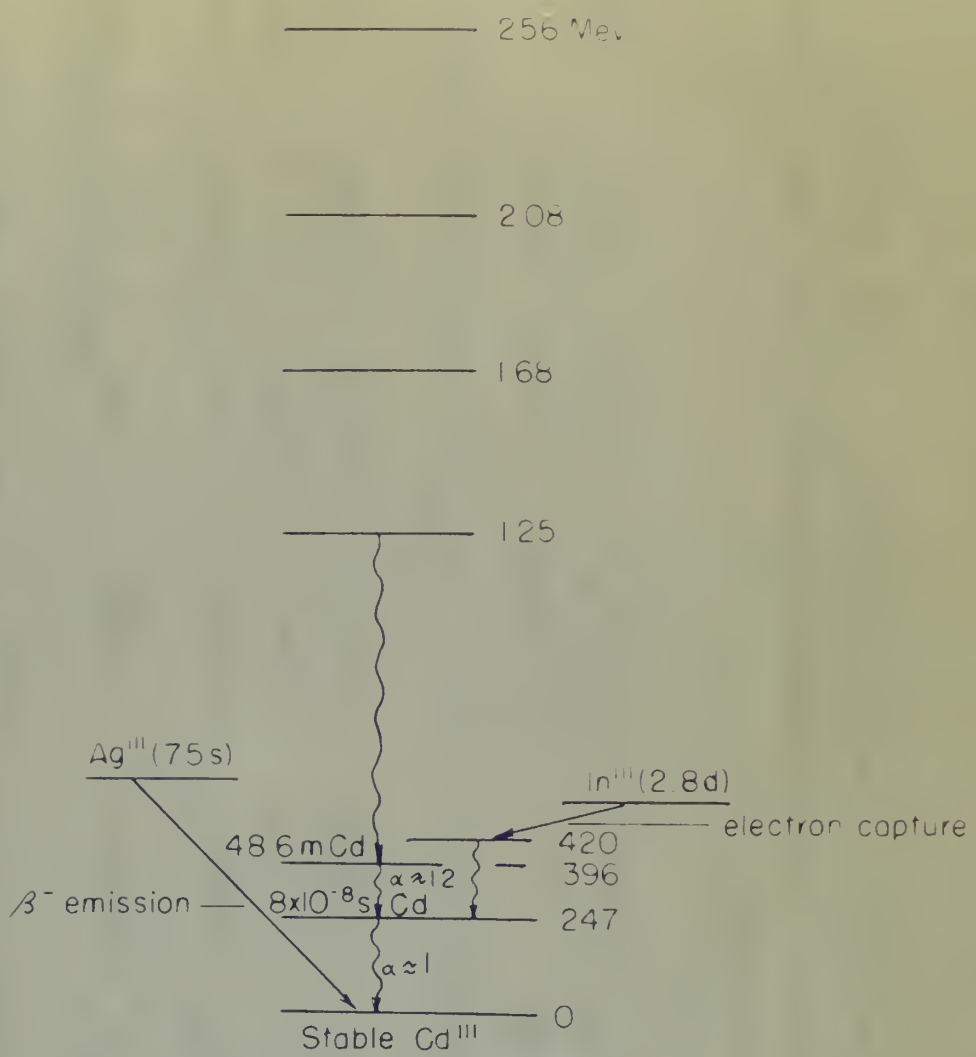

Spin = ½ Abundance = .128

α = conversion coefficient

Figure 4

ENERGY LEVEL DIAGRAM FOR Cd^{111}

TABLE I

Cd^{111} E_γ = 0.149 Mev *α = 12 $T_{1/2exp.}$ = 48.6 min. Half-life units = minutes

	Theoretical				Corrected for Internal Conversion			
** Λ	Bethe(S3)	Lowen(M1)	Berthelot(M1)	Moon(M1)	Bethe	Lowen	Berthelot	Moon
3	4.82×10^{-3}	9.20×10^{-6}	1.15×10^{-6}	2.99×10^{-5}	3.71×10^{-4}	7.07×10^{-7}	8.86×10^{-8}	2.30×10^{-6}
4	1.39×10^{4}	1.79x10	3.42×10^{-1}	5.75x10	1.07×10^{3}	1.38	2.63×10^{-2}	4.42
5	6.98×10^{10}	6.07×10^{7}	1.92×10^{5}	very long	5.37×10^{9}	4.67×10^{6}	1.48×10^{4}	very long

Cd^{111} E_γ = 0.247 Mev *α = 0.1 $T_{1/2exp.}$ = 8×10^{-8} sec. Half-life units = seconds

2	2.48×10^{-8}	5.97×10^{-11}	---	1.16×10^{-10}	2.26×10^{-8}	5.42×10^{-11}	---	1.05×10^{-10}
3	2.20×10^{-2}	2.65×10^{-5}	3.00×10^{-6}	6.95×10^{-5}	1.00×10^{-2}	2.41×10^{-5}	2.72×10^{-6}	6.32×10^{-5}

*α = Internal conversion coefficient.

**Order of electric multipole = Λ, order of magnetic multipole = Λ - 1 (Magnetic 2^{ℓ}-pole radiation has approximately the same probability of occurring as electric $2^{\ell+1}$-pole radiation.)

[illegible]

[illegible]

[illegible]

A comparison of the experimentally determined 48.6-minute half-life of the 0.396-Mev level with the theoretical half-lives corrected for internal conversion indicates quite clearly that the transition from this level to the 0.247-Mev level is by electric 2^4-pole or magnetic octupole radiation ($\Lambda = 4$). The assignment of $\Lambda = 4$ to the 0.149-Mev transition coincides with the multipole order designated by Helmholtz, Hayward, and McGinnis (H5) and by Axel and Dancoff (A1) for this transition. A similar comparison for the transition from the 0.247-Mev level to the ground state ($T_{1/2\ exp.} = 6 \times 10^{-8}$ second) indicates that Λ is 2 or 3, but does not allow a reliable assignment of a specific value to .

A knowledge of the half-life alone does not allow determination of whether a gamma-ray transition involves an electric or a magnetic multipole, but a comparison of experimentally obtained K or L conversion coefficients or the K/L ratio of the coefficients with theoretically calculated values of the same quantities may facilitate such a determination. Table II gives currently accepted experimental and calculated theoretical data concerning internal conversion for probable values of Λ for transitions from both metastable states in Cd^{111}. The theoretical values were calculated from formulas developed by Dancoff and Morrison (D1) or were obtained from tables or graphs, based on these formulas, prepared by Hebb and Nelson (H6). Table II indicates with reliable certainty that the transition from the 48.6-minute level is by electric 2^4-pole radiation (the same assignment has been made by Helmholtz et al. (H5)). If the transition from the 6×10^{-8}-second level is of

TABLE II

DATA ON INTERNAL CONVERSION OF Cd^{111}

		Experimental	Theoretical	
			Electric	Magnetic
E_γ = 0.149 Mev Λ = 4.00	a_K	7.72	5.63	3.40
	a_L	4.28	6.05	0.66
	a_K/a_L	1.80	0.906	5.08
E_γ = 0.247 Mev Λ = 2.00	a_K	0.09	0.0394	0.015
	a_L	0.01	0.00584	0.0021
	a_K/a_L	10.00	6.74	7.22
E_γ = 0.247 Mev Λ = 3.00	a_K	0.09	0.117	0.077
	a_L	0.01	0.0165	0.0112
	a_K/a_L	10.00	6.31	6.90

a_K = K shell internal conversion coefficient.

a_L = L shell internal conversion coefficient.

Table XI

Data on Chemical Composition of PS_{XIX}

the $\Lambda = 3$ type, Table II indicates that it is probably by magnetic quadrupole radiation, but if $\Lambda = 2$, the table fails to indicate specifically whether the transition is by electric quadrupole or magnetic dipole radiation. The difficulty of assigning the correct multipole order to this transition is emphasized by the contradictory reports in the recent literature concerning this transition (D2, K1, K5).

A metastable state is defined as any excited state having a measurable lifetime. Weizsacker showed that assigning an angular momentum to the metastable state differing by 3 to 5 units from the angular momentum of the state of lower energy to which the metastable state decays by gamma-ray emission justifies theoretically its observable lifetime. Instrumentation and measuring techniques have improved so much since Weizsacker suggested his hypothesis that decays of excited states with very short lifetimes are now detectable. Therefore, isomers which have recently been (5×10^{-8} second Cd^{111}) or in the near future will be reclassified as metastable may have angular momentum differences less than 3, because of their very short lifetimes.

Figure 5 shows all the possible combinations of angular momentums for the ground and metastable states of Cd^{111} for those decay schemes which are indicated by a comparison of theory and experiment.

[illegible] $V = 3$ [illegible] [illegible] [illegible]

$\Delta_{2-1}=4$ $\Delta_{1-0}=2$ $E_{2-1}=0.149$Mev 2^4-pole electric

$E_{1-0}=0.247$Mev 2^2-pole electric

	Energy	Parity	Possible Values of Angular Momentum
I_2	0.396	±	$*\frac{13}{2}$ $\frac{11}{2}$ $\frac{9}{2}$ $\frac{7}{2}$ $\frac{5}{2}$ $\frac{3}{2}$ $\frac{11}{2}$ $\frac{9}{2}$ $\frac{7}{2}$ $\frac{5}{2}$
$\Delta=4$			
I_1	0.247	±	$\frac{5}{2}$ $\frac{5}{2}$ $\frac{5}{2}$ $\frac{5}{2}$ $\frac{5}{2}$ $\frac{5}{2}$ $\frac{3}{2}$ $\frac{3}{2}$ $\frac{3}{2}$ $\frac{3}{2}$
$\Delta=2$			
I_0	0	±	$\frac{1}{2}$ $\frac{1}{2}$ $\frac{1}{2}$ $\frac{1}{2}$ $\frac{1}{2}$ $\frac{1}{2}$ $\frac{1}{2}$ $\frac{1}{2}$ $\frac{1}{2}$ $\frac{1}{2}$

$\Delta_{2-1}=4$ $\Delta_{1-0}=2$ $E_{2-1}=0.149$Mev 2^4-pole electric

$E_{1-0}=0.247$Mev 2^1-pole magnetic

	Energy	Parity	Possible Values of Angular Momentum
I_2	0.396	±	$*\frac{11}{2}$ $\frac{9}{2}$ $\frac{7}{2}$ $\frac{5}{2}$ $\frac{9}{2}$ $\frac{7}{2}$
$\Delta=4$			
I_1	0.247	±	$\frac{3}{2}$ $\frac{3}{2}$ $\frac{3}{2}$ $\frac{3}{2}$ $\frac{1}{2}$ $\frac{1}{2}$
$\Delta=1$			
I_0	0	±	$\frac{1}{2}$ $\frac{1}{2}$ $\frac{1}{2}$ $\frac{1}{2}$ $\frac{1}{2}$ $\frac{1}{2}$

$\Delta_{2-1}=4$ $\Delta_{1-0}=3$ $E_{2-1}=0.149$Mev 2^4-pole electric

$E_{1-0}=0.247$Mev 2^2-pole magnetic

	Energy	Parity	Possible Values of Angular Momentum
I_2	0.396	±	$*\frac{13}{2}$ $\frac{11}{2}$ $\frac{9}{2}$ $\frac{7}{2}$ $\frac{5}{2}$ $\frac{3}{2}$ $\frac{11}{2}$ $\frac{9}{2}$ $\frac{7}{2}$ $\frac{5}{2}$
$\Delta=4$			
I_1	0.247	±	$\frac{5}{2}$ $\frac{5}{2}$ $\frac{5}{2}$ $\frac{5}{2}$ $\frac{5}{2}$ $\frac{5}{2}$ $\frac{3}{2}$ $\frac{3}{2}$ $\frac{3}{2}$ $\frac{3}{2}$
$\Delta=2$			
I_0	0	±	$\frac{1}{2}$ $\frac{1}{2}$ $\frac{1}{2}$ $\frac{1}{2}$ $\frac{1}{2}$ $\frac{1}{2}$ $\frac{1}{2}$ $\frac{1}{2}$ $\frac{1}{2}$ $\frac{1}{2}$

* Most Probable Combination.

Figure 5

Method of Obtaining the Uncorrected Excitation Curve

Whether a detectable amount of activity of a metastable state may be excited or not depends on the cross section for the formation of the metastable state by the particular type of excitation process employed. The cross section for the formation of a metastable state by the inelastic scattering of neutrons is usually very small. The ease with which the decay of a metastable state may be detected depends on the energies of the gamma rays and electrons emitted during the decay and on the sensitivity of the detection equipment. Therefore, high backgrounds or substantial amounts of interfering radioactivities cannot be tolerated. Possible sources of background during this investigation were stray radiation from nuclear machines, sources, etc., cosmic radiation, light leaks, and thermal emission in the photomultiplier tube itself. Prior to the actual experiment, considerable time was spent in reducing to a minimum the amount of background available to the crystal and the phototube of the scintillation counter. Interfering radioactive decays, which may accompany the decay of the metastable state, result from nuclear reactions initiated in the impurities or other isotopes present in the sample by the bombarding neutrons.

The differential discriminator was especially applicable for use as a counter in this experiment because it counts only activity of the particular energies to which its window is sensitive. It

Control of Circulation and Respiratory Centers

Although a distinction cannot be drawn between the
above and the material in the three preceding chapters, it
is convenient to treat the circulation and respiration as
separate topics. The former section deals with the
mechanical aspects of the circulatory system, the latter
with the nervous mechanisms that control the rate of
breathing. The nerve centers that regulate the diameter of a
particular vessel, for example, are considered in the
section on circulation, while those that control the rate
of respiratory movements are discussed in the latter
section. Therefore, blood pressure is considered
with circulation. Chemoreceptors are discussed in connection
with respiration, although they are important in
controlling the rate of heart beat. Pulse is
considered with circulation, although it is determined by a
combination of factors. Intermittent positive pressure
breathing, which may accompany the use of the respirator and the
physiology of the ventilation apparatus, is considered in
connection with the mechanics of breathing in the respiratory
section. Anesthesia is considered in relation to
circulation and respiration.

The circulatory disturbances and cardiac emergencies
that may be a concern in this experimental procedure are
discussed in the section on pathophysiology.

was five times less sensitive to background than an Atomic Instrument decade scaler, when both instruments were counting the same background simultaneously.

The experimental samples were made from high-purity commercial cadmium sheet manufactured by the Belmont Smelting and Refining Company, of Newark, New Jersey. A spectroscopic analysis of this cadmium indicated that it contained about 0.1 per cent copper and 0.1 per cent lead, but no impurities were present in sufficient quantities to interfere with detecting the decay of the metastable state. Unfortunately, the isotope, Cd^{111}, is only 12.8 per cent abundant in natural cadmium. Table III contains data on all the stable isotopes of cadmium and gives the nuclear reactions which can occur when these isotopes are subjected to bombardment by neutrons of the energies used in this experiment. Decay of Cd^{107} and Cd^{109} is not important because the per cent abundance of Cd^{106} and Cd^{108} in natural cadmium is so low. No reaction between Cd^{112} and neutrons of moderate or lesser energies has been observed. Cd^{112} and Cd^{114} are stable nuclides, so no further nuclear reactions result from neutron capture by Cd^{111} and Cd^{113}. Therefore, the only possible reactions which may interfere with detection the decay of metastable $^{*}Cd^{111}$ formed from stable Cd^{111} are:

(a) The formation of metastable $^{*}Cd^{111}$ from capture of fast neutrons by Cd^{110}.

(b) The formation of metastable $^{*}Cd^{113}$ from inelastic scattering of fast neutrons by Cd^{113}.

TABLE III

ISOTOPES OF CADMIUM

Per Cent Abundance	Isotope	Reaction	Half-Life	Decay Radiations
1.1	Cd^{106}	$Cd^{106} + n \rightarrow Cd^{107}$	6.7 hours	K, γ(0.546), β^+(0.32)
0.9	Cd^{108}	$Cd^{108} + n \rightarrow Cd^{109}$	1.3 years	K
12.4	Cd^{110}	$Cd^{110} + n \rightarrow {}^*Cd^{111}$	48.6 minutes	γ(0.149) I.T. e^-, γ(0.247) I.T. e^-
12.8	Cd^{111}	$Cd^{111} + n \rightarrow {}^*Cd^{111} + n$	48.6 minutes	γ(0.149) I.T. e^-, γ(0.247) I.T. e^-
24.1	Cd^{112}	---	---	---
12.3	Cd^{113}	$Cd^{113} + n \rightarrow {}^*Cd^{113} + n$	2.3 minutes	I.T. e^-
		$Cd^{113} + n \rightarrow Cd^{114}$	Stable	---
28.8	Cd^{114}	$Cd^{114} + n \rightarrow Cd^{115}$	2.33 days	β^-(0.6, 1.13), γ(0.52)
			43.0 days	β^-(1.67), γ(0.5)
7.6	Cd^{116}	$Cd^{116} + n \rightarrow Cd^{117}$	2.83 days	β^-(1.5)

Notes: (1) Decay radiations are in energy units of Mev.
(2) I.T. designates isomeric transition.
(3) e^- designates internal conversion.
(4) * designates excited state.

(c) The formation of unstable Cd^{115} and Cd^{117} from capture of fast neutrons by Cd^{114} and Cd^{116}.

(d) The formation of $*Cd^{111}$, Cd^{115}, or Cd^{117} by capture of thermal neutrons.

Ways of proving that these interfering reactions are unimportant or of correcting for their effect will be described in later sections of this chapter.

Figure 6 shows the experimental arrangement used for irradiating the cadmium samples. The 48.6-minute half-life of the 0.396-Mev metastable state in Cd^{111} permitted locating the counting equipment remote from the site of the irradiation. Figure 7 shows the setup of the scintillation counter and its associated electronic equipment used for detecting the decay of the 48.6-minute metastable state.

The long half-lives of some of the unstable isotopes of cadmium which result from neutron capture prevented reusing a sample until approximately two weeks after a previous irradiation. The 25 samples used during the investigation were cadmium disks 3 cm. in diameter and 1.626 mm. thick. The mass of the disks varied between 10.015 and 10.045 grams. Relatively heavy disks were used rather than light, thin foils, in order to insure the production of a significant amount of activity, even though the cross section for the formation of the metastable state was very small.

During those experimental runs which were used to obtain the excitation curve, the disk was positioned by an aluminum holder with its

Figure 6. Arrangement for irradiating the cadmium disks, showing the magnet and chamber of the Rockefeller generator, the tantalum-backed lithium target and the aluminum disk holder.

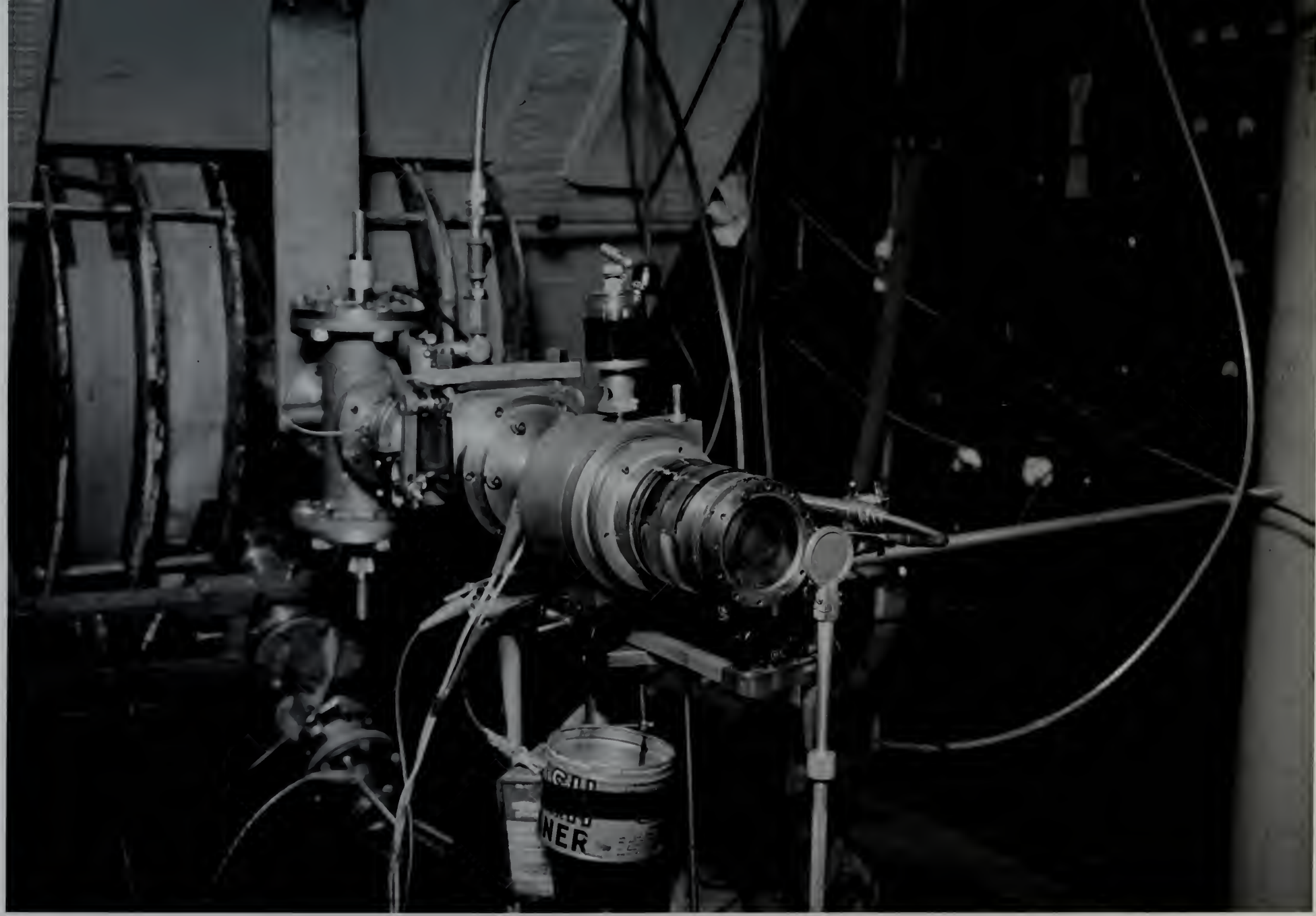

Figure 7. Setup of equipment used for detecting the decay of the metastable state, showing the high-voltage power supply, voltage stabilizer, lead-sheathed scintillation counter, cathode-follower pre-amplifier, amplifier, differential discriminator, and decade scaler.

Figure 7. Setup of equipment used for determining the power
of the measurable state, showing the high-voltage power supply, variable-
attenuator, input-terminal calibration counter, pushpull-pulsers pre-
amplifier, amplifier, differentiated discriminators, and dynode supply.

was operated at 1050 volts, and the coarse and fine gain settings of the amplifier were 9 and 7, respectively. The operation of the amplifier in conjunction with the differential discriminator was improved by adding a one-microsecond delay line clipper to the amplifier circuit. Preliminary experiments indicated that this combination of adjustments to the counting equipment gave the maximum ratio of desired decay counts to background counts. The window of the differential discriminator was adjusted to count preferentially the decays of $^{*}Cd^{111}$ and to discriminates as much as possible against any other interfering decays. The actual width and location of the window were such that all pulses between 6 and 28 volts were counted. The activity produced in the sample increased as the energy of the bombarding neutrons increased, and the number of background counts varied from 50 per cent to 4 per cent of the total counts, depending on the activity of the sample. The number of scintillation-counter counts occurring during the 45-minute counting period was recorded for each sample.

The induced activity in the sample (scintillation-counter counts/long-counter counts) was plotted against the maximum energy of the neutrons traversing the sample during an irradiation. This neutron-excitation curve is shown in Figure 8. The portion of the curve below a neutron energy of 0.8 Mev has been adjusted, as indicated by Figure 3, for the decrease of long-counter sensitivity at these lower energies. The swift rise of the curve at energies just above the neutron energy associated with the lithium threshold may be due to the decrease in

center in line with and perpendicular to the proton beam and at a distance of 4 cm. from the lithium target. The holder was made from aluminum because aluminum is almost completely transparent to neutrons of all energies. The disks were irradiated for periods of one hour with monoergic neutrons of various energies obtained from the $Li^7(p,n)$ reaction using a 60 Kev thick target on the Rockefeller generator. Fifteen minutes after the end of the irradiation, the radioactive decays occurring in the disks were counted in the scintillation counter.

If the different points on the excitation curve are to have comparative values relative to each other, the neutron flux traversing the sample must be uniform over the entire period of each irradiation. Several times during this investigation the Rockefeller generator operated unsatisfactorily and the proton beam was unstable and sporadic. Runs which were marred by lengthy interruptions of the neutron flux were of little value.

The relative number of neutrons traversing the sample for the different points on the excitation curve was determined by the long counter described in a previous section. The counter was set up one meter from the target and at zero degrees to the proton beam. The number of long-counter counts occurring during each irradiation was recorded.

Fifteen minutes after the end of the irradiation, the decays occurring in the sample were counted for a period of 45 minutes by the scintillation counter. During this investigation, photomultiplier tube

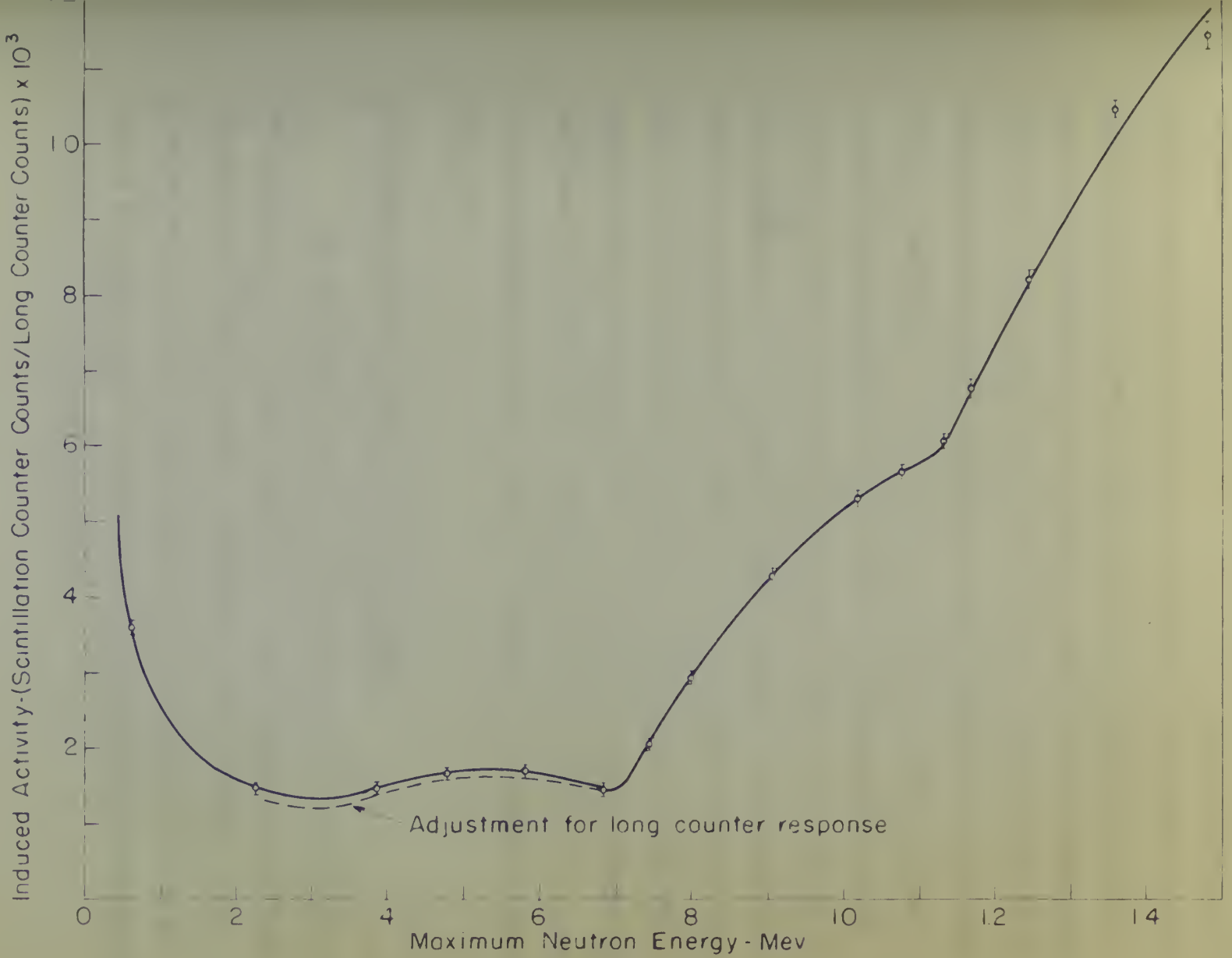

Figure 8

NEUTRON EXCITATION CURVE FOR $^{*}Cd^{111}$ UNCORRECTED

long-counter sensitivity at very low energies, a region about which Figure 3 gives no information. Alternatively, it may be due to a sharp increase in the cross section for neutron capture by some of the cadmium isotopes at very low neutron energies. Since this condition occurs at neutron energies well below the energy of the 48.6-minute metastable state, resolution of the question is not pertinent to the investigation of the metastable state. The statistics encountered in obtaining the data for the excitation curve represent an average uncertainty of 2 per cent in the value of the ordinate. The significance of the two sharp changes in the slope of the curve will be discussed after the curve has been corrected for interfering decays and for the neutron energy spread resulting from the finite target thickness, angularity, etc. The existence of these breaks in the curve was confirmed with certainty by the fact that their location was reproduced by a second set of data obtained three months after the first set.

Elimination of the Effect of Interfering Decays

The 15-minute interval between the end of the irradiation and the beginning of the 45-minute counting period allowed any 2.3-minute metastable ^{113}Cd to decay to a negligible amount before the actual counting was started and also provided the time necessary for transporting the sample from the target room of the Rockefeller generator to the location of the counting equipment.

The shape of the fundamental excitation curve between neutron energies of 0.3 and 0.7 Mev raises a suspicion that the curve really represents the sum of several activities with different half-lives. Therefore, an irradiation identical to those described in the previous section was made, and the decay of the sample was followed until the activity was decreasing at a very slow and uniform rate. Figure 9 is a graph of the total activity of the sample against the time after the end of the irradiation plotted on semi-log coordinates. The decay graph of an activity with a single half-life should be a straight line when plotted on such coordinates. The curvature of the plot confirms the suspicion that the total activity consists of two or more separate activities with different half-lives. According to the previous section, the possible components of the total activity are 48.6-minute $^{m}Cd^{111}$, 2.33-day Cd^{115}, 43-day Cd^{115}, and 2.8-hour Cd^{117}.

Since no activity was observed in the sample two weeks after the irradiation, the existence of the 43-day activity was ruled out. The shape of the decay curve 20 hours after the end of the irradiation was what would be expected for the decay of the 2.33-day activity alone. This activity was subtracted graphically from the total decay curve. The slope of the right-hand portion of the resulting curve confirmed the presence of the 2.8-hour activity. Separation of the 2.8-hour activity in a similar manner revealed that the remaining activity decayed with a 48.6-minute half-life. This graphical method of half-life separation is illustrated in detail in Figure 9.

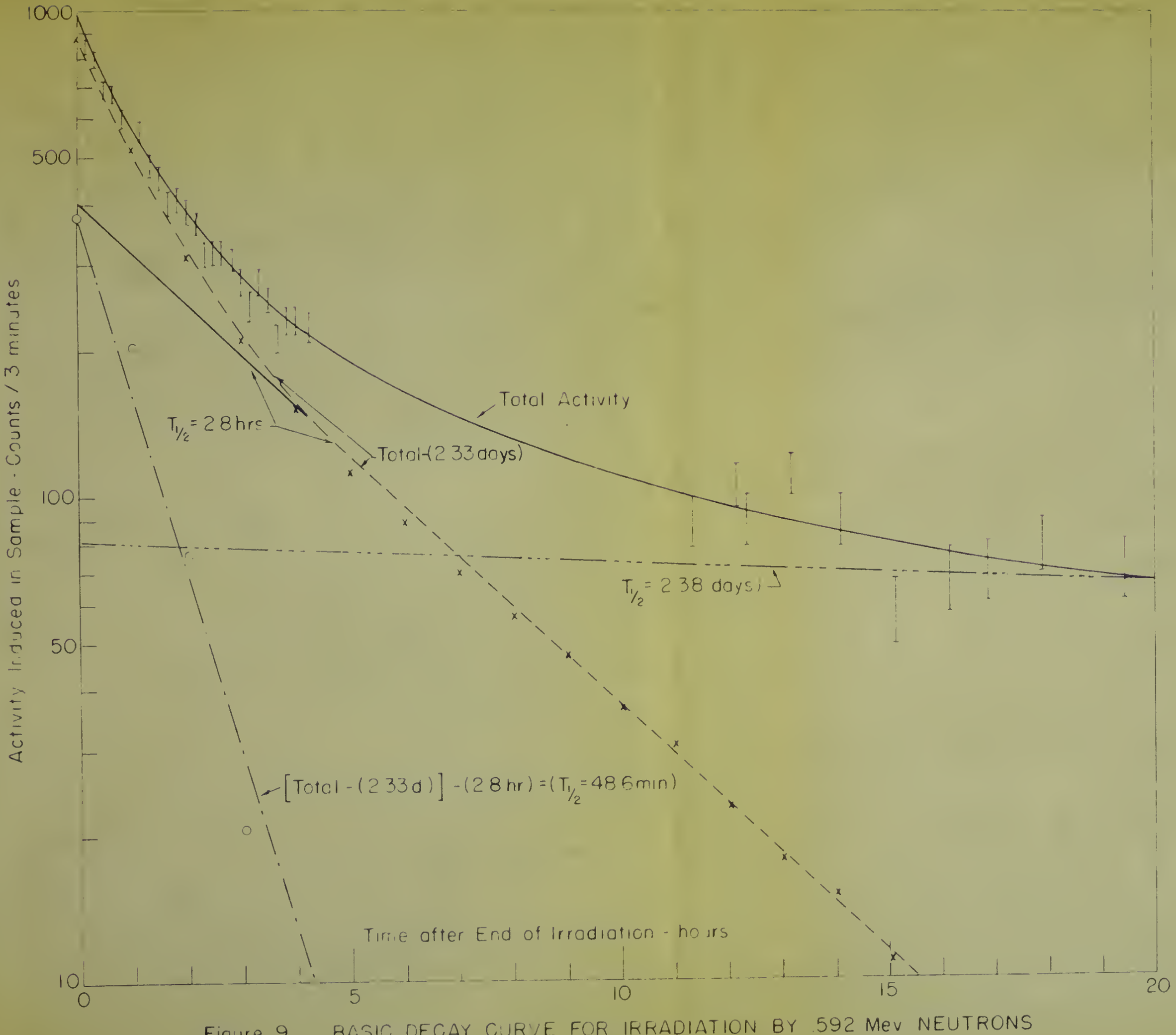

Figure 9 BASIC DECAY CURVE FOR IRRADIATION BY .592 Mev NEUTRONS

Sixteen additional irradiations were made throughout the range of neutron energies covered by the uncorrected excitation curve of Figure 8. Since radioactivity decays according to an exponential law, the amount of activity remaining five half-lives after its production is a negligible fraction of its initial value. Therefore, the amount of 46.6-minute activity remaining six hours after the end of the irradiation is negligible and the amount of 2.8-hour activity remaining 19 hours later is also negligible. The decay curves for each irradiation were extrapolated to zero time, and the total activity was read from them at 0, 6, and 25 hours after the end of the irradiation. Since it has been definitely established that only three separate activities exist, the knowledge of the total activity at these three times affords a means of computing mathematically the initial induced activity for each separate half-life. Next, the appropriate Bateman equation for each radioactive decay was integrated between the limits of 15 and 60 minutes. The total number of decays of each activity occurring in the 45-minute counting period was obtained by substituting the specific values of initial activity in the proper equations. Finally, this information was used to express the integral quantity of each separate activity as a fraction of the total activity observed during the 45-minute counting period. Figure 10 shows the varying shape of the total decay curves for substantially different fractions of 46.6-minute activity.

activity.

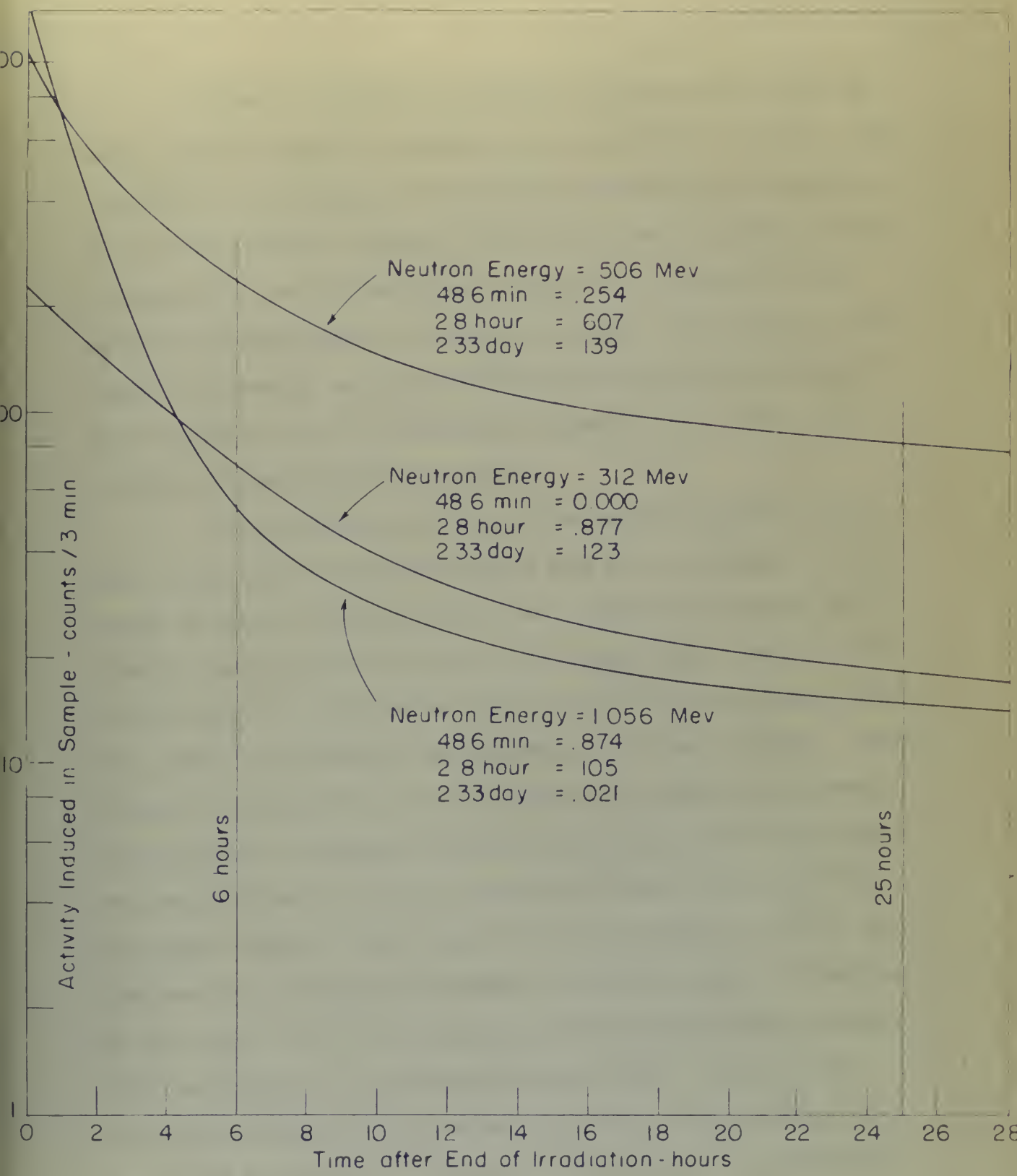

Figure 10

COMPARISON OF DECAYS FOR DIFFERENT %'s OF 486 MINUTE ACTIVITY

Figure 11 contains the separated excitation curves for the three different activities detected by the scintillation counter. The magnitude of each activity was obtained by multiplying the ordinates, at the proper neutron energies, from the fundamental excitation curve of Figure 8 by the fractional values calculated for each of the 17 half-life separation runs. The probable error in the ordinates of the curves of Figure 11, which is primarily due to the poor statistics at the low-activity end of the half-life separation decay curves, is estimated as approximately 5 per cent.

The possibility that some of the activity detected may be due to the capture of thermal neutrons must not be overlooked. The source of thermal neutrons could be the multiple scattering of fast neutrons from the walls and floor of the target room. Dempster (D4) has determined by mass spectrography that Cd^{113} is the isotope of cadmium mainly responsible for the absorption of thermal neutrons. Meyer, Peters, and Schmidt (M2) have also reported that their cross-section determinations for enriched cadmium isotopes indicatesthat absorption of thermal neutrons by all the isotopes of cadmium except Cd^{113} is negligible compared to the capture of thermal neutrons by Cd^{113}. The previous section has already pointed out that the capture of neutrons of any energy by Cd^{113} is unimportant to this investigation, because Cd^{114} is stable and no interfering decays result. The conclusion that the capture of thermal neutrons in general is unimportant was reaffirmed experimentally during this investigation. An irradiation

Figure 11 contains the experimental resistivity curves for the three different resistivity fractions of the metallization mixture. The magnitude of each resistivity was obtained by multiplying the resistance, as the probe contacts overlapped, first the full-film cross-section, then the theoretical resistance curves of figure 9 by the fractional volume occupied by the 17 parts-film cross-section. The logarithmic nature of the ordinates of curves of figure 11, which is necessary due to the great resistivities at low-metal and of the parts-film cross-section, is emphasized by plotting.

The possibility that some of the resistivity determined may be due to the existence of thermal resistance must not be overlooked. The source of thermal resistance could be the multiple constriction of heat lines from the metal and flower of the heated areas. Thompson (19) has determined by some approximations that CR_{113} is the inverse of mechanical possibility for the dissipation of thermal resistance. However, Peters, and Dahnke (20) have also indicated that their cross-section determinations for restricted contact flatness indicated dissipation of thermal resistance by all the junctions of metallic powder CR_{113} is negligible compared to the product of thermal resistance by CR_{113}. The previous section has clearly pointed out that the resistance of each junction by CR_{113} is restricted to their thermalization. However CR_{113} is simply not an independent design element. The connection that the existence of thermal resistance is determined by the magnitude of the resistivity during this investigation. We importation

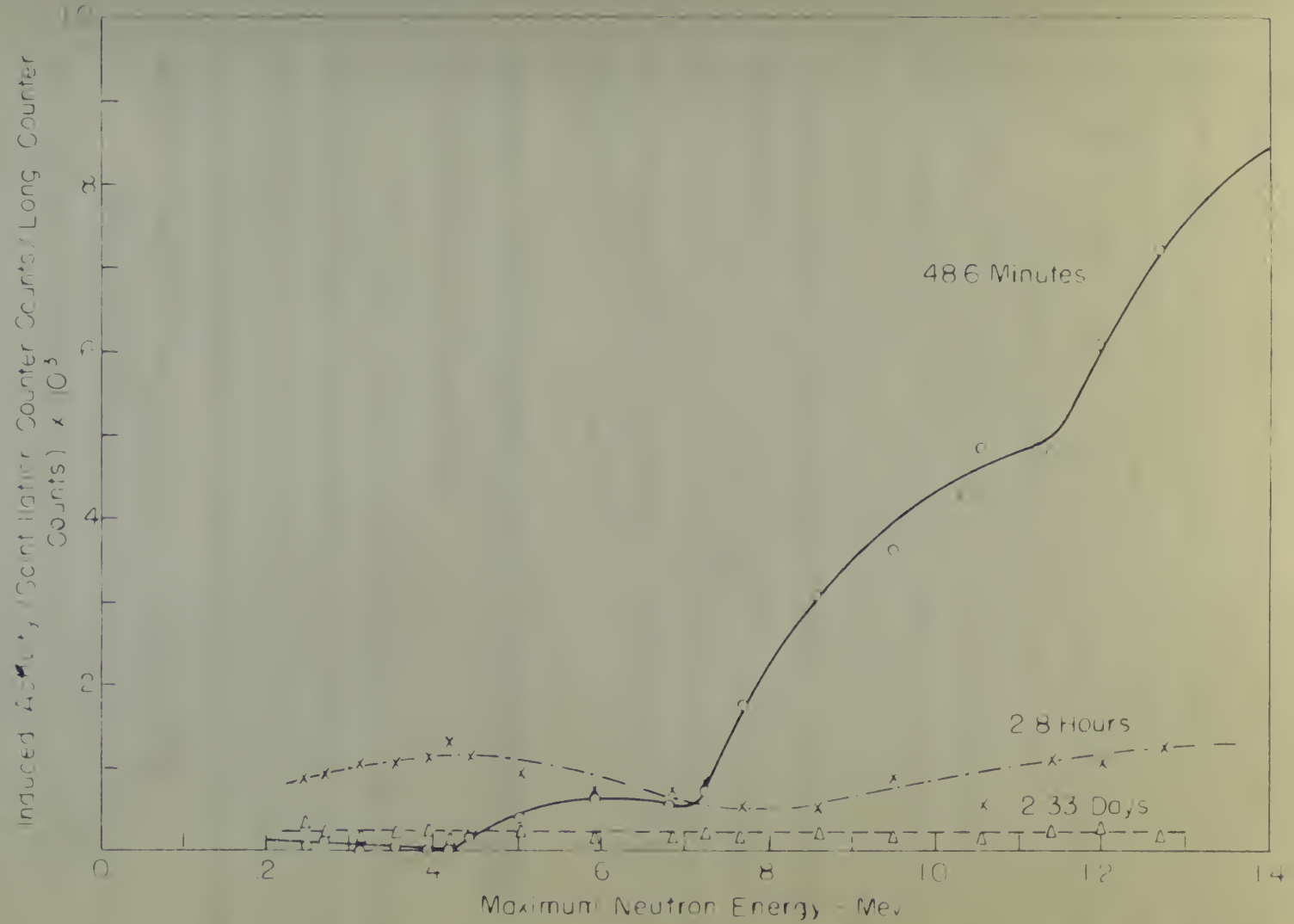

Figure 11

EXCITATION CURVES FOR THE SEPARATED ACTIVITIES OF $^{*}Cd^{111}$, Cd^{115}, and Cd^{117}

was made on a sandwich of three identical cadmium disks. Decay curves for an outer disk which was exposed to any background of thermal neutrons which may have existed in the target room and for the center disk which was shielded from such a background were equal within statistics.

An accurate determination of whether any of the 48.6-minute metastable Cd^{111} was being formed by the absorption of fast neutrons in Cd^{110}, instead of by the inelastic scattering of fast neutrons by Cd^{111}, was impossible. However, the relatively small amounts of 2.8-day and 2.33-hour activities observed and the dearth of the 48.6-minute activity in the vicinity of a 0.4-Mev neutron energy indicates that the cross section for this capture reaction is very small in an energy range covered by this investigation. Therefore, the effect of neutron capture by Cd^{110} has been neglected.

Correction of the 48.6-Minute Excitation Curve for Proton-Energy Spread, Target Thickness, and Angularity

The energy resolution of the abscissas of the excitation curves obtained during this investigation may be affected by three factors: fluctuations in the energy of the proton beam, the thickness of the lithium target, and the dependence of neutron energy on the angle of neutron emission relative to the direction of the proton beam.

During this experiment, the Rockefeller generator was operated with a total exit slit opening of one mm. Such an adjustment of the beam defining slits, together with other characteristics of the generator

which contribute slightly to fluctuations in the proton energy, causes a spread in the energy of the protons striking the lithium target of less than 5 kilovolts. The spread in neutron energy resulting from this resolution in proton energy relative to the spread in neutron energy caused by other reasons is very small. In fact, it is probably smaller than the probable error in the determination of the thickness of the lithium target. Therefore, its effect has been neglected.

Because of the low cross section for the formation of the metastable state, it was necessary to use a thick lithium target and to place the sample close to the target, in order to excite a significant amount of activity in the sample. This procedure involves a sacrifice in the resolution of the energy of the neutrons traversing the sample.

A target with a thickness equivalent to 60 kilovolts of proton energy was used to obtain the excitation curve shown in Figure 8. The method of determining the target thickness is described in Chapter III. The neutrons produced in a target of finite thickness follow a rectangular number-energy distribution. The average spread in neutron energy resulting from the 60-kilovolt target (expressed in proton energy) is 50 kilovolts.

The 3-cm. cadmium disks were located 4 cm. from the lithium target during the irradiations. With the sample at this position, all the neutrons emerging from the target between the angles of 0 and 20.6 degrees strike it. The spread in neutron energy, due to emission angle,

varies from 25 kilovolts at a neutron energy of 0.4 Mev to 40 kilovolts at 1.4 Mev.

In Figures 8 and 11, the activity induced in the samples is plotted against the maximum energy of the neutrons producing it. It is desirable to correct these curves so that the induced activity is plotted against the mean energy of the neutrons producing it. Willard's (W6) curves of neutron yield from the $Li^7(p,n)$ reaction versus angle of neutron emission indicate that the yield is nearly constant for angles up to 20 degrees in the energy range of this investigation. Therefore, it was assumed that the neutron flux was uniform over the whole angle at the target intercepted by the sample when making this correction.

In the following discussion, the total neutron energy spread due to target thickness is represented by ΔE_p and that due to the solid angle intercepted by the sample by ΔE_θ. The actual values of ΔE_p and ΔE_θ, for the energy range covered in this experiment, were calculated with the aid of a table, "Neutron Energy as a Function of Proton Energy and Angle for the $Li^7(p,n)Be^7$ Reaction," prepared by Willard (W6).

Let it be assumed that the cross section for the formation of the metastable state is constant over the energy spread, ΔE_θ, and that the neutron beam is monoergic at zero degrees ($\Delta E_p = 0$). Then, as the angle at the target increases, the increment of annular area on

value from 25 minutes to a certain energy of 0.8 how do the different
at 1.2 MeV.

In Figures 8 and 11, the activity induced in the sulphur is
plotted against the neutron energy of the neutrons producing it. It
is desirable to present these curves so that the INDUCED ACTIVITY is
plotted against the NEUTRON ENERGY of the neutrons producing it. Hilsch's
(16) measure of neutrons yield from the $Li^7(p,n)$ reaction versus angle
of neutron emission indicate that the yield is nearly constant for
angles up to 30 degrees in the energy range of this investigation.
Therefore, it was assumed that the neutrons flux was uniform over the
whole angle at the target intercepted by the sample when making this
measurement.

In the following discussion, the total neutron energy spread
due to target thickness is represented by ΔE_T and that due to the
solid angle intercepted by the sample by ΔE_Ω. The actual values of
ΔE_T and ΔE_Ω for the energy range covered in this experiment, were
calculated with the aid of a table, "Neutron Energy as a Function of
Proton Energy and Angle for the $Li^7(p,n)Be^7$ Reaction," prepared by
Hilsch (16).

Let it be assumed that the error function for the distribution
of the neutrons which is produced over the energy spread, ΔE_T and
that the neutrons then is observed at some degrees ($\Delta E_\Omega = D$). Then,
as the angle at the energy increases, the increment of energy over an

the sample, associated with a specific increment of ΔE_θ, also increases. Therefore, the number of neutrons of a specific energy striking the sample increases as the angle at the target increases and the neutron energy decreases. The mean neutron energy, considering energy dependence on angle only, is rigorously calculated to be $\left[E_{max} - 0.71\,\Delta E_\theta\right]$. The scintillation counter, because of geometry, counts the decays occurring near the outside of the sample less efficiently than those occurring at the center of the sample. This tends to counteract the effect described above, and the mean energy of the effective neutrons may be taken as approximately: $\left[E_{max} - 0.5\,\Delta E_\theta\right]$.

Then the total correction to be subtracted from E_{max}, assuming a rectangular number-energy distribution for the spread of neutron energy due to target thickness, is approximately: $\left[0.5\,\Delta E_p + 0.5\,\Delta E_\theta\right]$. McCue (M3) has derived a formula which includes secondary effects due to changing curvature for making this type of correction. The simplification of McCue's formula, shown below, gives an approximate, but convenient, method of making the desired correction to the neutron excitation curve.

$$A'(E_{mean}) = 4/3\,A(E_{max}) - 1/6\,A(E_{max} + \delta) - 1/6\,A(E_{max} - \delta)$$

E_{max} = maximum neutron energy read from Figure 11.

$$\delta = 0.5\,\Delta E_p + 0.5\,\Delta E_\theta \ .$$

$A(X)$ = induced activity for energy X read from Figure 11.

$E_{mean} = E_{max} - \delta$ = mean neutron energy on corrected excitation curve.

$A'(E_{mean})$ = induced activity for mean neutron energy on corrected excitation curve.

The use of the above approximation is justified because it involves only a slight deviation from the true correction, which is a small per cent of the total induced activity. This correction does not apply at the thresholds for the formation of the metastable state and higher excited levels (indicated by sharpchanges in the slope of the excitation curve) or in the energy interval equal to $[\Delta E_p + \Delta E_\theta]$ above these thresholds. When the maximum neutron energy is just equal to the threshold energy, the correction must be zero because only neutrons with the threshold energy are contributing to the excitation. At an energy $[\Delta E_p + \Delta E_\theta]$ above the threshold, all the neutrons striking the sample are potentially effective, and the correction becomes applicable. In the region where the correction, according to the above formula, is not applicable, the true correction is very complicated and depends on the fraction of all the neutrons striking the sample which is effective in causing excitation, as well as on ΔE_p and ΔE_θ. The amount of experimental data obtained in these critical regions was insufficient to allow making an accurate correction to these portions of the uncorrected excitation curve of Figure 11.

McCue's simplified formula was applied to the excitation curve of Figure 11, except in the critical regions above the three thresholds. In these regions, the correction varies from zero at the threshold to the magnitude given by the formula at an energy of ($\Delta E_p + \Delta E_\theta$) above the threshold. The corrected curve is shown in Figure 12. The shape of the curve in the uncertain regions above the thresholds has been estimated by extrapolating the known portions of the curve back to the threshold energies. From the cross-section standpoint, the most important part of the excitation curve is between the threshold for the formation of the metastable state and the first excited level above it. Since this portion of the curve is relatively flat, a slight error in the shape of the curve just above the threshold is not very serious. It should be noted that the threshold and the excited levels occur at the same energies on both Figure 11 and Figure 12.

The corrected excitation curve indicates that the threshhold for exciting the metastable state is 400 ± 25 Kev. The presence of excited levels at 720 ± 20 Kev and at 1.15 ± 0.02 Mev is also evident. The errors assigned above are due to uncertainty in determining the target thickness, in correcting for interfering half-lives, target thickness, etc., and in drawing the curve itself.

Determination of the Absolute Cross Section for Formation of the Metastable State

A knowledge of the absolute cross section for the formation of the metastable state may facilitate assignment of a value to l ,

of the metastable state was investigated as a means to l.

A knowledge of the absolute cross section for the formation

Differential Yield

Differentiation of the Expression Giving Yield as a Function of the

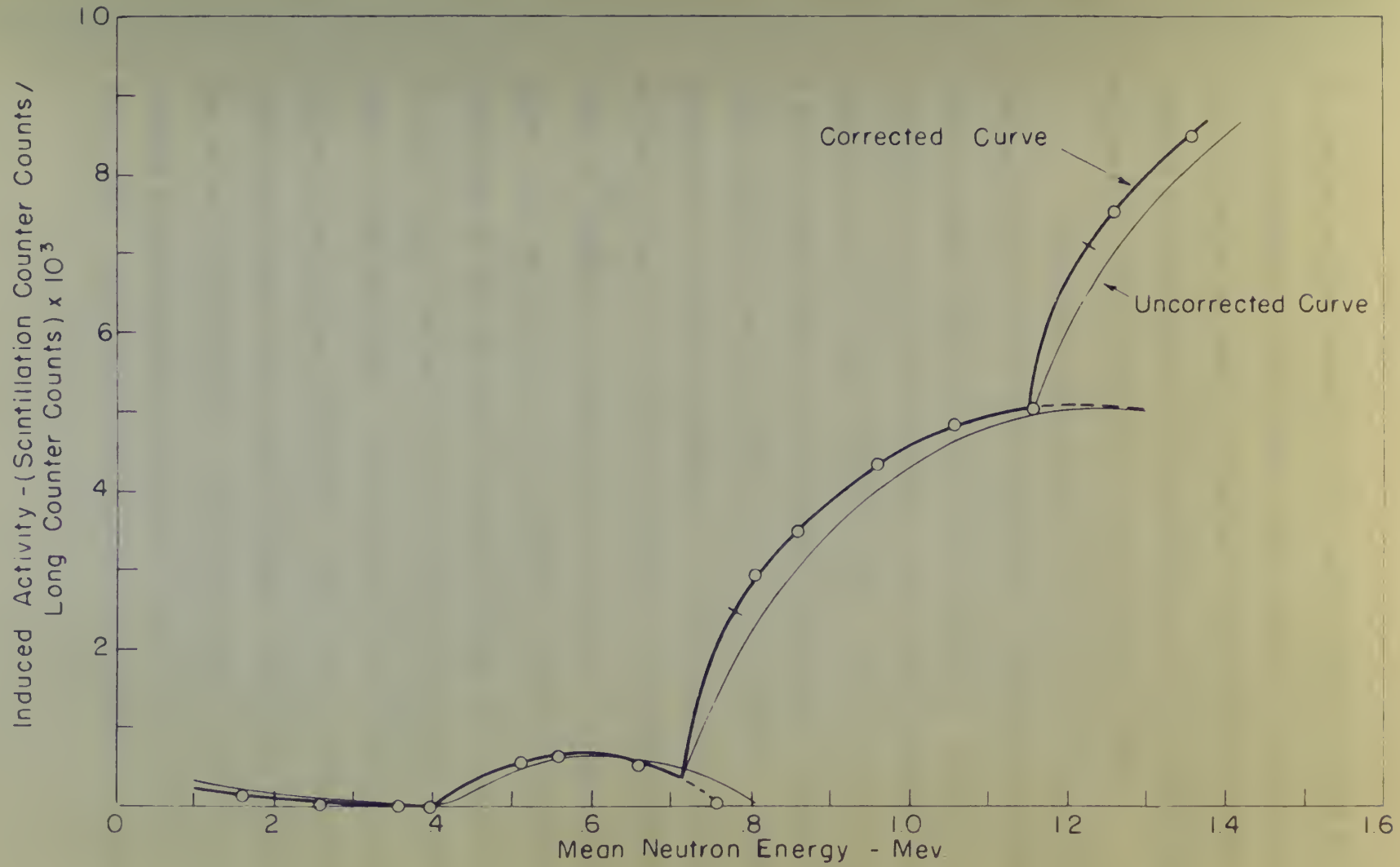

Figure 12

EXCITATION CURVE FOR 48.6 METASTABLE $^{*}Cd^{111}$ CORRECTED FOR FINITE TARGET THICKNESS AND ANGULARITY OF INCIDENT NEUTRONS

the orbital angular momentum of the neutron which excited the state. The determination of this cross section from the experimental data already obtained requires a knowledge of the absolute neutron flux incident on the sample and of the efficiency of the scintillation counter for counting the decay of the metastable state.

The absolute neutron flux was determined for one point on the excitation curve by utilizing Hanson, Taschek, and Williams' (H7) data on neutron yield from the $Li^7(p,n)$ reaction. A sample was irradiated for one hour with neutrons from a 3.1-Mev proton beam incident on a 30-kilovolt lithium target. Hanson et al. report that a 3.1-Mev proton beam on a 40-kilovolt target yields 4.3×10^6 neutrons per microcoulomb per unit solid angle at zero degrees. Assuming that the yield is directly proportional to target thickness at this energy, the yield during the one-hour irradiation of the cadmium sample was 3.2×10^6 neutrons per microcoulomb per unit solid angle at zero degrees. The total number of microcoulombs recorded by the beam current integrator of the Rockefeller generator during this run was 20630 . The solid angle intercepted by the 3-cm. diameter disk located 4 cm. away is 0.396 steradians. Therefore, 2.61×10^{10} neutrons traversed the sample during the irradiation. This sample was also counted in the scintillation counter for 45 minutes, starting 15 minutes after the end of the irradiation. The induced activity for this run, expressed as scintillation-counter counts per incident neutron was 7.56×10^{-7}. The induced activity from the excitation curve of

Figure 12 for the same mean neutron energy, 1.357 Mev, is 8.48×10^{-4} scintillation-counter counts per long-counter count. The curve of Figure 12 may be normalized to give induced activity in terms of scintillation-counter counts per incident neutron by multiplying its ordinates by the ratio $(7.56 \times 10^{-7}/8.48 \times 10^{-4}) = 8.92 \times 10^{-4}$.

The resolving time of the scintillation counter was not short enough to discriminate between the decay of the 45.6-minute metastable state and the decay of the 8×10^{-8}-second metastable state. Therefore, each transition from the 0.396-Mev level to the 0.247-Mev level is accompanied by a simultaneous transition from the 0.247-Mev level to the ground state. Both gamma-ray transitions are partially internally converted. All the possible radiations available to the counter from this decay scheme are listed below:

(a) 0.149-Mev unconverted gamma ray.

(b) 0.123-Mev conversion electron.

(c) 0.247-Mev unconverted gamma ray.

(d) 0.221-Mev conversion electron.

(e) 0.026-Mev cadmium X-ray.

The 0.149-Mev gamma ray is 92.25 per cent internally converted ($\alpha = 12$) and the 0.247-Mev gamma ray is 9.09 per cent internally converted ($\alpha = 0.1$) (M1). The range of the 0.221-Mev electrons in cadmium is 0.005 cm. and the sample disks were 0.1625 cm. thick. Therefore, only the 0.005 cm. layer on the outside of the disk toward the counter is effective in emitting electrons, and the number from

this source is negligible. The 0.123-Mev electrons have a much shorter range, so their effect is even more negligible. The self absorption of the X-rays, 0.149-Mev gamma rays, and 0.247-Mev gamma rays in the cadmium disk is 94 per cent, 40 per cent, and 20 per cent, respectively. A comprehensive treatment of all the nuclear data given above indicates that 86 per cent of all the radiation emitted during the decay of metastable Cd^{111} is 0.247-Mev unconverted gamma rays. Since the counter efficiency probably increases with increasing gamma-ray energy, the 0.247-Mev gamma ray may be an even greater fraction of the total effective radiation. Therefore, in determining the efficiency of the scintillation counter, it will be assumed that only the 0.247-Mev gamma rays are counted. Of course, the total number of counts recorded by the scintillation counter includes 1.5-Mev beta rays from the decay of 2.8-hour Cd^{117} and 0.6-Mev beta rays, 1.13-Mev beta rays and 0.52-Mev gamma rays from the decay of 2.33-day Cd^{115}, as well as the radiation from the decay of metastable $*Cd^{111}$. Part of the unwanted radiation from Cd^{115} and Cd^{117} is excluded by the window of the differential discriminator and the remainder has been separated from the radiation emitted by decaying metastable $*Cd^{111}$ by the half-life-separation method already described in a previous section.

Hg^{203} decays with a 43-day half-life by emitting a 0.210-Mev beta ray and a 0.279-Mev gamma ray. This isotope was readily available at the time of this investigation. Since it emits a

single gamma ray of nearly the same energy as the 0.247-Mev gamma ray from metastable $^{*}Cd^{111}$ and also has a relatively long lifetime, Hg^{203} was chosen as a standard for estimating the efficiency of the scintillation counter for detecting the decay of metastable $^{*}Cd^{111}$. Some Hg^{203} was sealed between two lucite disks, 3 cm. in diameter and 1/16 inch thick. The uniform distribution of the Hg^{203} between the disks gave approximately the same counting geometry as that of the cadmium samples. The lucite completely absorbed the beta rays. The method of determining the absolute rate of gamma-ray emission by the standard is described in Appendix B.

At the time the efficiency of the scintillation counter was determined, the Hg^{203} standard emitted 1.107×10^{5} gamma rays per second. The activity of the standard, the minimum acceptable to the platinum-screen gamma-ray counter used for standardization, was sufficient to jam the register of the differential discriminator. Therefore, an Atomic Instrument Company Model 105 decade scaler with a conventional discriminator was used with the scintillation counter for the efficiency determination. The Hg^{203} standard emitted 2.98×10^{6} gamma rays during a 45-minute counting period, and the decade scaler actually recorded 1.672×10^{6} counts during this time. This gives a counter efficiency of 0.56 per cent. Since the differential discriminator was used for the experimental runs, this figure must be corrected to take into account the radiation which is excluded by its window, and a correction must also be made for the radiation which is self-absorbed in the cadmium sample.

The electron field, crystal, etc., of the metallizing-
material tend to give the ligand rearranged by the differential steer-
ability of the double bonding a distribution of energies, even though
the common ring modified by the negative ion energy. The double
bonding is essential in all the problems in this energy distribution,
but the number of the nitro-methyl thermodynamic modulation part of
time. A single one was made or a Cp_2^{3d} energies above both the nitro-
methyl electrolyzation and the double nuclear were in the metallization-
reverse element of the room time. This was instructed that the dif-
ferential electrolyzation accounted only 77 per cent of the energy
required by the double nuclei. Though for each of the O_2SH-ion
gamma ring then the theory of Cd-complex metabolite $^{cd}_{333}$ are nuc-
absorbed in the negative itself. Therefore, the over-all efficiency
for counting the O_2SH-ion gamma ray from these metabolite $^{cd}_{333}$ is 0.3
per cent.

The validity of the source of Figure 12 may be accounted as
metastable change per lantanum ammine if it is ionized by the meta-
phosphate positron-ion neutralization fusion and divided by the meta-
bifluoride-reverse effluent.

A nine direct procedure for determining the absolute number
of metastable isomers would have been for:

(a) Count the isomers in a machine specific rise & negative
ionization run with the double action.

(b) Determine the absolute number of decays for this specific run by applying the efficiency obtained with the decade scaler and the Hg^{203} standard.

(c) Enter the curve of Figure 12 at the mean neutron energy used in (a) and normalize the curve to the absolute value determined in (b).

The above procedure was not used because the window of the differential discriminator excludes a large part of the unwanted activity from the decay of Cd^{115} and Cd^{117}, which is counted by the decade scaler.

The cross section for formation of the metastable state was computed by use of the following formula:

$$\frac{I_0 - I}{I_0} = 1 - e^{-n\sigma t} .$$

I_0 = neutrons incident on the sample.

I = neutrons which traverse the sample without exciting the metastable state.

$I_0 - I$ = neutrons exciting the metastable state.

n = the number of scattering nuclei per cm^3 of sample.

σ = cross section for formation of the metastable state.

t = thickness of the sample.

The appropriate calculation indicates that 0.363 of all the Cd^{111} nuclei excited to the metastable level during the irradiation

decay during the 45-minute counting period. Therefore, the quantity $(I_0 - I)$ also equals the absolute number of decays occurring during the counting period divided by 0.383. After final simplification:

$$\frac{I_0 - I}{I_0} = 0.686 \text{ x ordinate of Figure 12.}$$

Figure 13 is a graph of the cross section for formation of the metastable state plotted against the mean energy of the incident neutrons. The ordinate of this curve is subject to an estimated error of $\pm$ 25 per cent due to:

(a) The probable error in the ordinate of Figure 12.

(b) The uncertainty in the absolute rate of gamma-ray emission by the Hg^{203} standard.

(c) The assumption that the scintillation counter counts only the 0.247-Mev gamma ray from the decay of the metastable state in Cd^{111}.

(d) Error in determining the absolute neutron flux.

Comparison of the Theoretical and Experimental Cross Sections

A comparison of the experimental cross section for the formation of the metastable state with the theoretical cross section, $\sigma_c(l)$, for the formation of the compound nucleus, Cd^{112}, as a function of l for the incoming neutron allows the assignment of a maximum value to the orbital angular momentum the neutron can carry in. The quantity,

Figure 13

CROSS SECTION FOR FORMATION OF METASTABLE STATE IN Cd^{111}

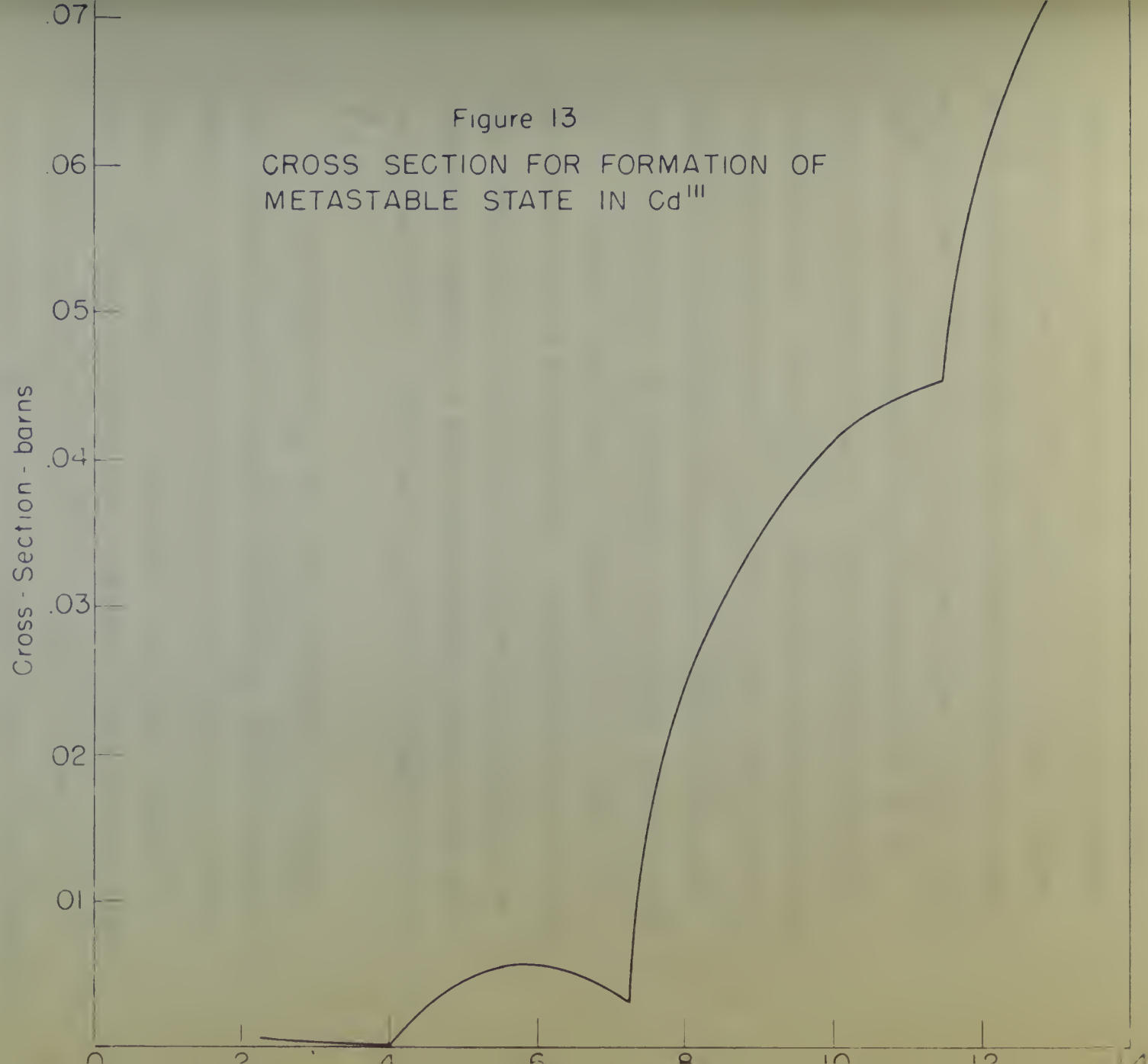

$\sigma_c(l)$, has been calculated following the method of Blatt and Weisskopf [3], as described in Chapter II, for the neutron-energy region from 0.2 Mev to 1.2 Mev for values of l from zero through 5. It should be noted that these calculations involve the kinetic energy of the neutron in the center of mass system. However, since Cd^{111} is a relatively heavy nucleus, the kinetic energy of the neutron is essentially the same in both the center of mass and the laboratory system. Those $\sigma_c(l)$'s which are in a range a few orders of magnitude above and below the experimental cross section for the formation of the metastable state are plotted against mean neutron energy in Figure 14. The experimental cross section in the vicinity of the threshold has also been plotted on the graph in Figure 14. The curves of Figure 14 are plotted on semi-log graph paper in order that a practical scale may be used for the vertical coordinate. An unqualified evaluation of these curves indicates that the most angular momentum which a neutron can carry into the compound nucleus is $l = 3$.

The formula for W_1, the fraction of nuclei decaying from the compound nucleus to a specific excited state, is also given in Chapter II. An inspection of the formulas for $\sigma_c(l)$ and W_1 shows that for the case of $l = 0$, the cross section $\sigma_c(0)$ decreases as $(E - E_{th})^{-1/2}$, and, therefore, the probability of decay to the specific state associated with W_1 increases as $(E - E_{th})^{1/2}$. When an $l = 1$ neutron is emitted in the decay of the compound nucleus, the probability of

$\alpha^{\beta}(l)$, has been estimated following the method of Stark and Weinhouse [32], as described in Chapter II, for the neutron-neutron reaction from 0.5 mev to 1.5 mev for values of l from zero through 3. It should be noted that these calculations involve the binding energy of the neutron in the nucleus of these atoms. However, since $d_{3/2}$ is a relatively loose neutron, the binding energy of the neutron is essentially the same in both the nucleus of mass and the laboratory system. Thus $\alpha^{\beta}(l)$'s which are in a range a few orders of magnitude above and below the experimental curve applied here mention changes in the resonable shape are plotted against mass neutron energy in Figure 13. The experimental curve results in the velocity of the threshold has also been plotted on the graph in Figure 13. The curves of Figure 13 are plotted on semi-log graph paper in order that a practical scale may be used for the vertical coordinate. An exponential variation of these curves indicates that the cosh expression which is contained within the square root sign in the expressed reaction is a constant. This may be used for the vertical coordinate. An exponential variation of these curves indicates that the cosh expression which is contained within the square root sign in the expressed reaction is a constant.

The formula for S^{l}, the fraction of neutral disrupting form the compound nucleus in a specific neutral state, is also given in Chapter II. An inspection of the formulas for $\alpha^{\beta}(l)$ and S^{l} shows that for the case of $l = 0$, the cross section $\alpha^{\beta}(0)$ decreases in $(3 - E^{\beta\beta})^{-1/2}$ and, therefore, the probability of decay to the specific state associated with S^{l} increases as $(3 - E^{\beta\beta})^{1/2}$. Then as $l = 1$

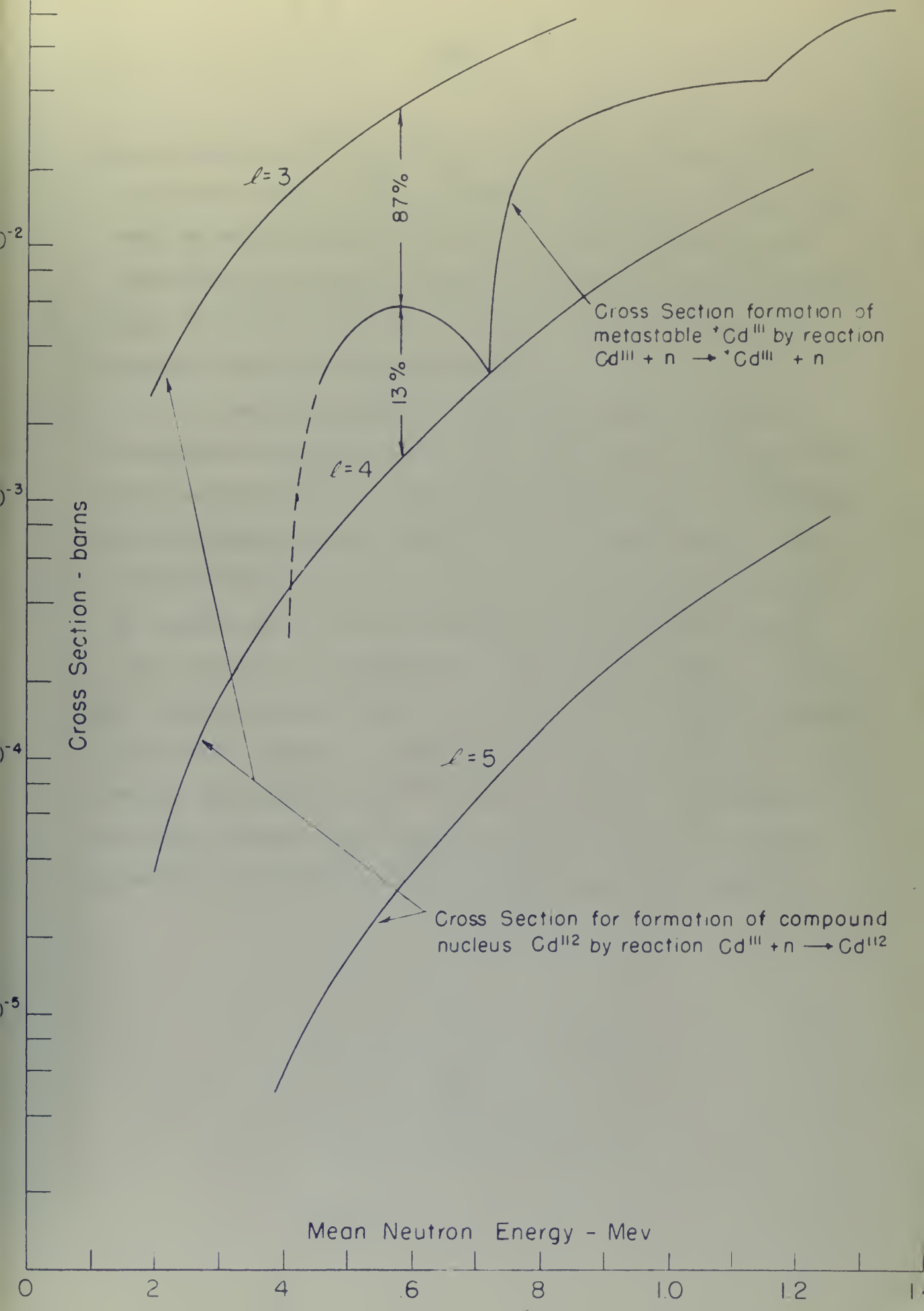
ℓ = 3
87%
13%
ℓ = 4
ℓ = 5
Cross Section formation of metastable *Cd111 by reaction Cd111 + n → *Cd111 + n
Cross Section for formation of compound nucleus Cd112 by reaction Cd111 + n → Cd112
Cross Section - barns
Mean Neutron Energy - Mev
0
2
4
.6
8
1.0
1.2

decay increases as $(E - E_{th})^{3/2}$ and, in general, as $(E - E_{th})^{(l+1/2)}$. A mathematical analysis of these formulas indicates that if the decay occurs by the emission of an $l = 0$ neutron, the curve of W_1 versus neutron energy approaches its threshold perpendicular to the horizontal axis. For the case of higher values, the curve approaches the threshold tangent to the horizontal axis.

When the experimental cross section for the formation of the metastable state is divided by the cross section for the formation of the compound nucleus, the resulting quantity is W_1, the probability that the compound nucleus will decay to the metastable state. Such a calculation was carried out using the experimental cross section for the formation of the metastable state and the theoretical value of $\sigma_c(3)$. The curve of W_1 versus mean neutron energy is shown in Figure 15. The shape of this curve in the vicinity of the threshold indicates that an $l = 0$ neutron is emitted from the compound nucleus. The curve deviates from the $(E - E_{th})^{1/2}$ curve as the neutron energy increases above the threshold value, because competition from decay to levels other than the metastable state commences as the energy increases.

either than the metastable state corresponds to the energy increment.

Above the dissociational cross section for the formation of the metastable state is divided by the cross section for the formation of the ionized molecule. The resulting quantity is P_i^J, the probability that the ionized molecules will decay to the metastable state. Such a calculation was carried out using the dissociational cross section for the formation of the metastable state and the Franck-Condon values of $\sigma_{ij}^0(J)$. The curve of P_i^J versus beam ambient energy is shown in Figure 15. The shape of this curve is the validity of the threshold indicates that as $\lambda = 0$ vanishes it existed from the ionizational conditions. The curve deviates from the $(E - E^{th})_{1/2}$ curve as the ambient energy increases above the threshold value, because contributions from decay to levels other than the metastable state commences as the energy increases.

A mathematical analysis of these formulae indicates that if the decay constant for the emission of an $\lambda = 0$ electron, the curve of P_i^J versus ambient energy approaches its theoretical dependence on the Boltzmann factor. For the case of higher values, the curve deviates the theoretical decay in the horizontal axis.

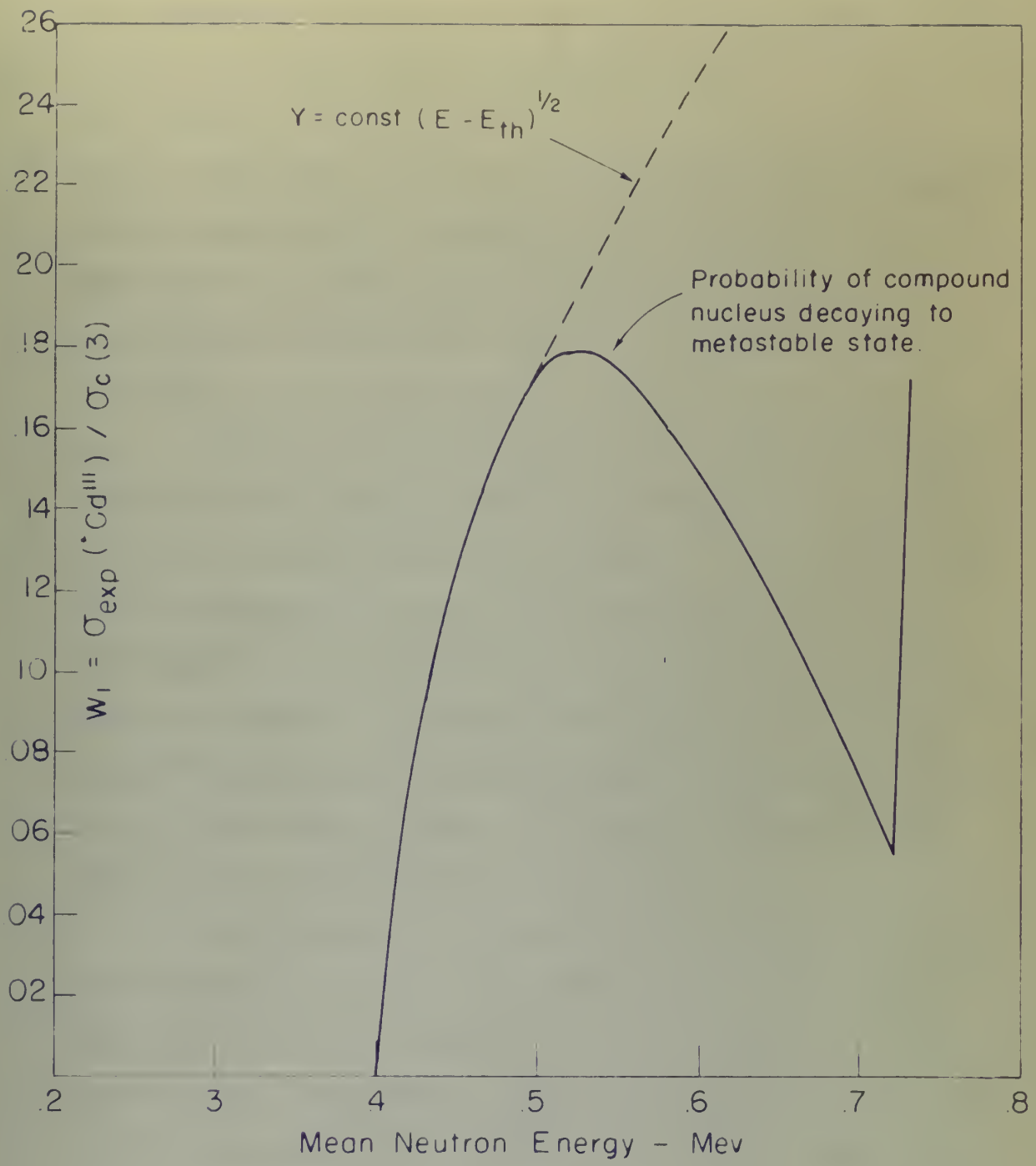
Y = const (E - E_th)^1/2
Probability of compound nucleus decaying to metastable state.
W_1 = σ_exp (*Cd^III) / σ_c (3)
26
24
22
20
18
16
14
12
10
08
06
04
02
.2
3
4
.5
.6
.7
.8
Mean Neutron Energy - Mev

Figure 15

V. CONCLUSIONS AND SUGGESTIONS FOR FURTHER INVESTIGATION

DISCUSSION AND SUMMARY OF RESULTS

The neutron excitation curve obtained during this investigation indicates that the threshold energy for the formation of the metastable state is 0.400 Mev and also reveals the existence of energy levels at 0.720 Mev and 1.150 Mev. The location of the metastable state is currently accepted as 0.396 Mev above the ground state. Therefore, the neutron excitation curve indicates the direct excitation of the metastable state. The existence of the 0.720-Mev energy level has not been reported previously. The 1.150-Mev energy level is probably the same one which Wiedenbeck (W7) obtained by both photon and electron bombardment and to which he assigned the energy of 1.250 Mev. The results of this investigation and those results obtained by Ebel (E1) indicate that neutron excitation gives slightly lower values of energy than photon or electron excitation gives for what are apparently the same levels.

The comparison of theoretical and experimental cross sections indicates that an $l = 3$ neutron forms the compound nucleus, which then emits an $l = 0$ neutron. If the metastable state is excited directly, conservation of angular momentum and parity for the above l values gives the metastable state a possible angular momentum of 9/2, 7/2, or 5/2 and a parity different than that of the ground state. According to Figure 5, the most probable value of

angular momentum for the metastable state, when its parity is different than that of the ground state, is 13/2 and the 0.149-Mev transition is by electric 2^4-pole radiation, while the 0.247-Mev transition is by magnetic quadrupole radiation. An angular momentum of 9/2, 7/2, or 5/2 for the metastable state is possible for this decay scheme, but much less probable than 13/2. The probability for the above possible values decreases rapidly as the magnitude of the angular momentum decreases.

Although the curve for the experimental cross section shown in Figure 14 is above the theoretical curve for $\ell = 4$, it is much closer to the curve for $\ell = 4$ than the curve for $\ell = 3$. After considering the uncertainties involved in determining the experimental cross section, it is conceivable that the experimental curve may be so much in error that its true position should be below the $\ell = 4$ theoretical curve. If this is the case, an $\ell = 4$ neutron excites the metastable state directly. If the points on the experimental cross section curve retain their relative positions and the curve, as a whole, is moved vertically downward until it is below the $\ell = 4$ theoretical curve, a new graph similar to the one in Figure 15 would still indicate that an $\ell = 0$ neutron is emitted by the compound nucleus. These new conditions would give the metastable state a possible angular momentum of 11/2, 9/2, or 7/2 and the same parity as the ground state. An angular momentum of 11/2 and no parity change are consistent and most probable, as shown in Figure 5, for the assignment of electric 2^4-pole radiation to the 0.149-Mev transition

and magnetic dipole radiation to the 0.247-Mev transition. The above values of angular momentum are also possible, but not probable, for the case where the 0.149-Mev transition is by electric 2^4-pole radiation and the 0.247-Mev transition is by electric quadrupole radiation.

McGinnis (34) has very recently stated that the 0.396-Mev level has an angular momentum of 13/2 and decays by electric 2^4-pole radiation to the 0.247-Mev level and that the 0.247-Mev level has an angular momentum of 5/2 and decays by electric quadrupole radiation. These assignments of spin and type of multipole give both metastable states the same parity as the ground state. His determinations are based on a comparison of experimental values of half-life, conversion ratios, etc., with theoretical relations presented in Rose's (31) tables for the K conversion coefficient. (Rose's tables were not available to the author until after the interpretation of the experimental results of this investigation had been accomplished). McGinnis's decay scheme is the one which the author initially considered most probable (see Figure 5), but unfortunately it does not agree with the most probable values of angular momentum indicated as possible by the experimental results of this investigation.

In^{111} decays by electron capture to a 0.420-Mev level in Cd^{111}. The probable error in the threshold energy obtained by this investigation for exciting the metastable state is of such magnitude that the excitation curve could be read to indicate the direct excitation of the 0.420-Mev level and its immediate decay to the metastable state. The presence of the 0.420-Mev level has only been observed in

connection with the decay of In^{111}. Attempts to separate any 48.6-minute metastable $^{m}Cd^{111}$ from decaying In^{111} have been unsuccessful (M4). McGinnis has assigned an angular momentum of 7/2 to this level and reports that it decays to the 0.247-Mev level by the emission of magnetic dipole radiation. If the 0.420-Mev level was excited directly during this investigation by an $l = 3$ neutron, the parity considerations of McGinnis's decay scheme for this level are not satisfied. Direct excitation of the 0.420-Mev level by an $l = 4$ neutron is consistent with parity considerations, but very improbable. Since the energy differential between the 0.420-Mev level and the 0.396-Mev level is so small, a transition from the 0.420-Mev level to the 48.6-minute metastable level is even more improbable. Therefore, it is very doubtful that the 0.420-Mev level was excited directly.

Figure 16 shows the most probable decay schemes of those considered possible as a result of this investigation.

Suggestions for Further Investigation

The neutron excitation curve should be extended to higher energies in order to confirm the energy levels at 1.68, 2.08, and 2.56 Mev obtained by Wiedenbeck (W7) from both photons and electron excitation.

It is planned to retain the experimental equipment, used during this investigation, intact for some time into the future. Therefore, it is recommended that additional experimental work be directed toward a better determination of the absolute cross section for the

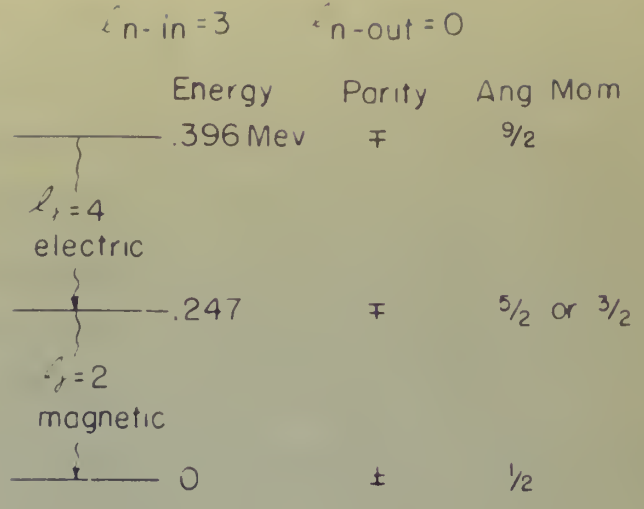

CASE I

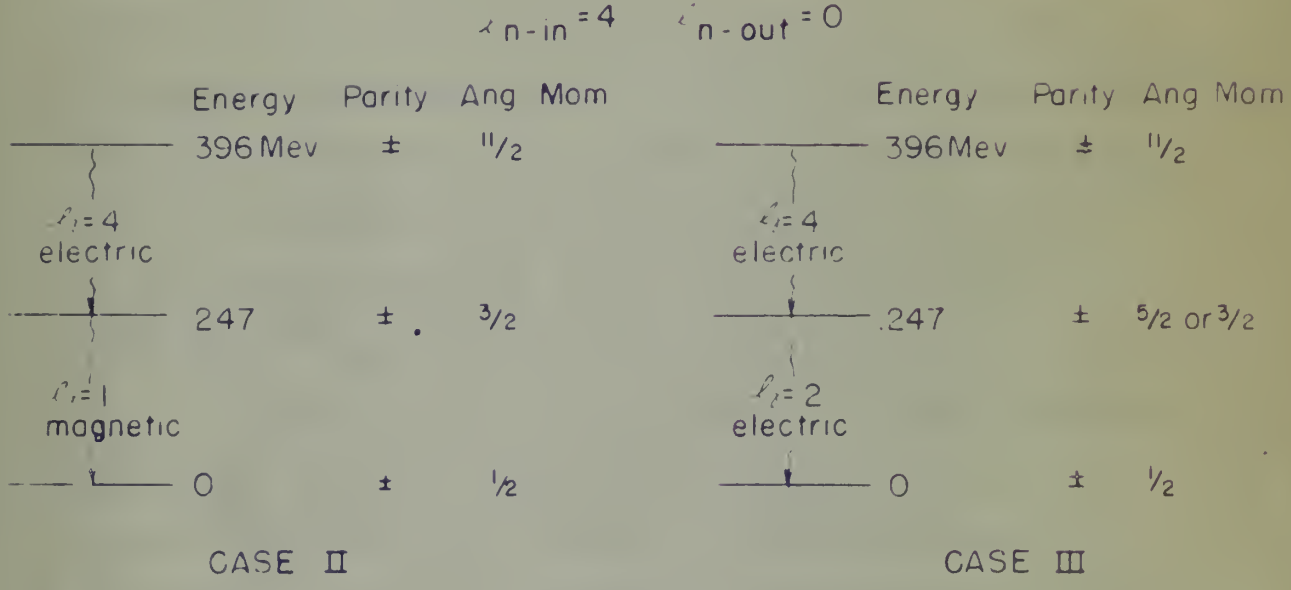

CASE II

CASE III

Figure 16

MOST PROBABLE ASSIGNMENT OF ANGULAR MOMENTUM AND PARITY TO THE METASTABLE STATE OF Cd^{111}.

formation of the metastable state. This effort should include a confirmation of the absolute neutron flux incident on the sample by a method independent of Hanson, Taschek and Williams (H7), a more accurate method of determining the efficiency of the scintillation counter, and a careful experimental analysis, by other means than half-life separation, of the different kinds of radiation detected by the counter during the decay of metastable $^{*}Cd^{111}$.

If the scintillation counter is moved to a location in the near vicinity of the target room of the Rockefeller generator, an investigation of the 2.3-minute metastable $^{*}Cd^{113}$, similar to the one described in this report, may be made. Because of the relatively short half-life of metastable $^{*}Cd^{113}$, the time required for irradiations and counting will be much less than that spent during the investigation of metastable $^{*}Cd^{111}$. The author has procured disks of barium peroxide which may be used for another similar investigation of the excitation of the 2.6-minute metastable state in Ba^{137} by fast neutron bombardment. It seems that the investigations of Cd^{113} and Ba^{137} could be conveniently carried on at the same time.

Appendix C contains a brief summary of several unsuccessful attempts to obtain neutron excitation curves for metastable states in various isomers. This work was carried on before the final selection of Cd^{111} as a subject for this investigation was made.

first estimates of ^{122}Cd as a subject for this investigation was made.

Attempts to obtain greater resolution during the determination of the absolute positron flux incident on the sample by a method independent of Curran, Dawson and Williams (17), a more accurate method of determining the efficiency of the scintillation counter, and a careful experimental analysis, by other means than half-life exploration, of the different kinds of radiation delayed by the neutron during the decay of radioactive ^{122}Cd.

If the scintillation counter is moved to a location in the near vicinity of the target room of the Berkeley cyclotron, an investigation of the 2.3-minute radioactive ^{119}Cd, similar to the one described in this report, may be made. Because of the relatively short half-life of radioactive ^{119}Cd, the time required for irradiation and counting will be much less than that spent during the investigation of radioactive ^{122}Cd. The method has presented itself of having pionetic which may be used for another similar investigation of the constituents of the 5.0-minute radioactive state in ^{119}Cd by fast neutron bombardment. It seems that the investigations of ^{122}Cd and ^{119}Cd might be conveniently carried on at the same time.

BIBLIOGRAPHY

A1 P. Axel and S. Dancoff, Phys. Rev. 76, 832 (1949(.

B1 S. W. Barnes and P. W. Aradine, Phys. Rev. 55, 50 (1939).

B2 H. Bethe, Rev. Mod. Phys. 9, 220 (1937).

B3 J. M. Blatt and V. F. Weisskopf, Laboratory for Nuclear Science and Engineering, M.I.T., Technical Report No. 42.

D1 S. M. Dancoff and P. Morrison, Phys. Rev. 55, 122 (1939).

D2 M. Deutsch and D. Stevenson, Phys. Rev. 76, 184 (1949).

D3 M. Deutsch and W. Wright, Phys. Rev. 77, 130 (1950).

D4 A. J. Dempster, Phys. Rev. 71, 144 (1947).

E1 A. A. Ebel, "Metastable States in Medium and Heavy Weight Nuclei," Ph. D. Thesis, M.I.T., (1950).

E2 W. C. Elmore and M. L. Sands, Electronics: Experimental Techniques, National Nuclear Energy Series V-1, (New York: McGraw-Hill Book Co., Inc., 1949).

G1 M. Goldhaber, R. D. Hill, and L. Szilard, Phys. Rev. 55, 47 (1939).

G2 M. Goldhaber and C. O. Muehlhause, Phys. Rev. 74, 1248 (1949).

H1 N. Hole, Arkiv. Mat. Astron. Fysik, 36A, No. 9, (1948).

H2 M. M. Hobb and G. E. Uhlenbeck, Physica 5, 605 (1938).

H3 F. A. Hadden, Ph. D. Thesis, M.I.T. (1950).

H4 A. Hanson and J. McKibben, Phys. Rev. 72, 673 (1947).

H5 A. Helmholtz, R. Hayward, and C. L. McGinnis, Phys. Rev. 75, 1469 (1949).

H6 M. M. Hobb and E. Nelson, Phys. Rev. 58, 489 (1940).

H7 A. Hansen, R. Taschek, and J. M. Williams, Rev. Mod. Phys. 21, 635 (1949).

BIBLIOGRAPHY

[1] P. Auer and E. Hagenauer, Proc. Amer. IEEE ICASSP (1994).

[2] M. E. Jaworska and P. E. Kandzia, Physics Lett. IEEE 20 (1970).

[3] E. Fermi, Elem. Nucl. Physics (Wiley 1972).

[4] H. H. Black and E. E. Voelcker, Laboratory for Insulator Research and Engineering M.I.T., Technical Report No. 10.

[5] R. M. Lancaster and P. Hargreaves, Progr. Nucl. Phys. IEEE (1972).

[6] R. Fowler and D. Hargreaves, Phys. Rev. IEEE (1948).

[7] P. Powell and H. Urbain, Proc. Lon. IEEE (1950).

[8] A. J. Dempster, Phys. Rev. IEEE (1947).

[9] A. A. Obed, "Materials Factor in Melting and Heavy Metals Design," M. S. Thesis, M.I.T., (1950).

[10] E. E. Moore and H. L. Cooke, Differential Thermal Analysis Fundamental Studies Using Basic Refractory Materials, Clay Expt. Station-Univ. Penn. Bull. No. 1944).

[11] C. Goldsmith, E. D. Ellis, and E. Berliner, Progr. Nucl. Phys. IEEE (1950).

[12] C. Goldsmith and E. E. Hollander, Phys. Rev. IEEE (1948).

[13] E. Segrè, Exptl. Nucl. Physics IEEE, No. 9, (1953).

[14] P. P. Ewald and E. E. Hollander, Physica IEEE (1930).

[15] R. W. Hamming (P. R. Bevels, M.I.T. 1950).

[16] E. Segrè and E. Hollander, Phys. Rev. IEEE, 673 (1947).

[17] E. Hollander, E. Segrè, and E. E. Hollander, Phys. Rev. IEEE 1948 (1948).

[18] P. P. Ewald and E. Hollander, Phys. Rev. IEEE 949 (1950).

[19] E. E. Moore and H. L. Williams, Nucl. Phys. IEEE 650 (1949).

J1 B. Jennings, Proc. I.R.E. 38, 1126 (1950).

L1 K. Lark-Horovitz, J. R. Risser, and R. M. Smith, Phys. Rev. 55, 575 (1939).

L2 I. Lowen, Phys. Rev. 59, 835 (1941).

L3 J. Lovington, M.S. Thesis, M.I.T. (1951).

M1 P. B. Moon, "Artificial Radioactivity," Cambridge University Press (1949).

M2 B. Meyer, B. Peters, and F. H. Schmidt, Phys. Rev. 69, 666 (1946).

M3 J.J.G. McCue, private communication.

M4 C. L. McGinnis, Phys. Rev. 81, 734 (1951).

N1 "Nuclear Data," NBS 499, National Bureau of Standards, U.S. Department of Commerce.

P1 W. M. Preston and Clark Goodman, Bul. Amer. Phys. Soc. 26, 29 (1951).

P2 W. C. Peacock, "A Study of the Absolute Efficiency of Gamma-Ray Counters with Application to Nuclear Spectroscopy," Ph. D. Thesis, M.I.T. (1944).

R1 M. E. Rose, G. H. Goertzel, W. I. Spinrad, J. Harr, and P. Strong, Phys. Rev. 76, 1853 (1949).

S1 G. T. Seaborg and I. Perlman, Rev. Mod. Phys. 20, 585 (1948).

S2 W. H. Sullivan, Trilinear Chart of Nuclear Species, (New York: John Wiley and Sons, 1949).

S3 E. Segre and A. C. Helmholtz, Rev. Mod. Phys. 21, 271 (1949).

S4 W. A. Schoenfeld and R. W. Duborg, M.S. Thesis, M.I.T. (1951).

T1 H. M. Taylor and N. F. Mott, Proc. Roy. Soc. A142, 215 (1933).

T2 R. Taschek and A. Hemmendinger, Phys. Rev. 74, 373 (1948).

W1 M. L. Wiedenbeck, Phys. Rev. 67, 92 (1945).

W2 M. L. Wiedenbeck, Phys. Rev. 67, 267 (1945).

12 T. Yamamoto, Proc. I.E.E.E. 55, 1345 (1967).

11 E. Lauterbrunnen, J. K. Gibson, and R. E. Smith, Phys. Rev. 55, 858 (1939).

10 I. Jones, Phys. Rev. 80, 1537 (1950).

9 J. Martindale, M.S. Thesis, M.I.T. (1952).

8 P. B. Moon, "Artificial Radioactivity," Cambridge University Press (1949).

7 E. Hooper, R. Peters, and T. E. Holmark, Phys. Rev. 60, 666 (1941).

6 A.A.S. Hughes, private communication.

5 E. F. Mahoney, Phys. Rev. 61, 174 (1942).

4 "Nuclear Data," NBS 500, National Bureau of Standards, U.S. Department of Commerce.

3 E. M. Freeman and Chien Shiung Wu, Rev. Mod. Phys. 25, 23 (1953).

2 E. C. Crawford, "A Study of the Absolute Activities of Cosmic-Ray Counters with Applications to Neutron Investigations," Ph. D. Thesis, M.I.T. (1948).

1 H. L. Jones, D. V. Osborne, C. E. Pollard, J. Kerr, and P. Sherman, Phys. Rev. 76, 1823 (1949).

0 T. Sanders and I. Fraenkel, Rev. Mod. Phys. 25, 838 (1953).

Ba E. E. Salpeter, Australian Journal of Scientific Research (Ser Europ Chem Nucl and Theor), 5(1952).

Be J. M. Blatt and V. F. Weisskopf, Theoretical Nuclear Physics, Ch. VIII (1952).

Bi M. A. Rothenstein and R. E. Taschek, Phys. Rev. 77, 803 (1950).

Bo N. Bohr, Nature 137, 344 (1936).

Br E. Brannen, H. I. S. Hudson, and J. S. Allen, Rev. Sci. Inst. 22, 574 (1951).

Ca J. Cassidy, Phys. Rev. 62, 52 (1942).

Ch G. L. Christofano, Phys. Rev. 61, 487 (1942).

W3 M. L. Wiedenbeck, Phys. Rev. 67, 53 (1945).

W4 M. L. Wiedenbeck, Phys. Rev. 68, 1 (1945).

W5 B. Walden and M. L. Wiedenbeck, Phys. Rev. 63, 60 (1943).

W6 H. B. Willard, "Interaction of Fast Neutrons with Nuclei," Ph. D. Thesis, M.I.T. (1950).

W7 M. L. Wiedenbeck, Phys. Rev. 66, 36 (1944).

ACKNOWLEDGMENTS

The graduate study of the author was sponsored by the Bureau of Ships and the U.S. Naval Postgraduate School. The work reported herein was undertaken in conjunction with the Nuclear Shielding Project of the Laboratory for Nuclear Science and Engineering, M.I.T., which project is sponsored by the Bureau of Ships and the Office of Naval Research.

The author wishes to express his appreciation to Dr. Clark Goodman, supervisor of this thesis, for his advice, interest, and constructive criticism during the progress of this research and the preparation of this thesis; to Dr. J.J.G. McCue for the unselfish contribution of a very large portion of his time to assisting with the experimental phases of this research and to making constructive criticisms during the preparation of this thesis; to Mr. Leonard Hubscher for many valuable discussions of theory; to Dr. Donald Stevenson and Mr. Marvin VanDilla for their suggestions on both the theory and the experimental procedure; to Dr. Paul Stelson, Mr. Donald Thompson, Mr. Ira Slawson, and Mr. John Adams for their aid in conducting the experiments at the Rockefeller generator; to Mrs. Evelyn McKinley for typing the manuscript; and to Mrs. Grace Rowe for reproducing the figures.

The preparation of the cadmium, rhodium, columbium, and mercury samples by Dr. T. S. Nagel, of the M.I.T. Metallurgical Project, is appreciated.

ACKNOWLEDGMENTS

The preparation of the machine was sponsored by the Bureau of Mines and the U.S. Naval Postgraduate School. The work described herein was undertaken in conjunction with the Student Scholarship Project of the Laboratory for Student Projects and Engineering, U.S.N., which project is sponsored by the Bureau of Ships and the Office of Naval Research.

The author wishes to express his appreciation to Dr. Clark Benson, supervisor of this thesis, for his advice, interest, and constructive criticism during the progress of this research and the preparation of this thesis; to Dr. U.S.N. Hardy for the meaningful completion of a very large portion of his time to consulting with the experimental phases of this research and in making constructive criticisms during the preparation of this thesis; to Dr. Leonard Richards for many valuable discussions of theory; to Mr. Donald Stevenson and Mr. Marvin Tuthill for their assistance on both the theory and the experimental phenomenon; to Dr. Paul Vatsaas, Dr. Donald Thornton, Mr. Jim Gibson, and Mr. John Adams for their aid in constructing the apparatus at the Postgraduate Laboratory in Inyo. Special gratitude for typing the manuscript, and to Mrs. Bruce Hess for reproducing the figures.

The permission of the captain, director, submitter, and secretary supplied by Lt. U. S. Engel, of the U.S.N. Postgraduate Project, is appreciated.

APPENDIX A

ALTERATION OF THE SINGLE-CHANNEL DIFFERENTIAL DISCRIMINATOR

The basic wiring diagram for the single-channel differential discriminator is the Laboratory for Nuclear Science and Engineering Drawing No. D-741-A, File 6420. This drawing calls for a 4700-ohm resistance in the plate circuit of the first tube of the discriminator which sets the low side of the window (6AC7). This resistance was reduced to 3700 ohms by placing an 15000-ohm resistance in parallel with the original 4700 ohms. This alteration reduced the hysteresis in the discriminator circuit; i.e., the signal voltage at which the discriminator recovered after being triggered was reduced. Such a change lowered the minimum setting at which the discriminator would operate.

APPENDIX A

ILLUSTRATION OF SOME ELECTRO-OPTICAL EXPERIMENTS

The basic optical diagrams for the single-channel electro-optical attenuator in the laboratory for Quantum Electronics and Spectroscopy (Section Tm. 8-Physik, ETH Zürich). This attenuator unit is for a Pockels-cell modulation in that light intensity of the first beam of the Glan-Thompson polarizer (Glan) into the two sides of the wedges (Quartz). This modulation was finished by placing an INDOC-cube polarizer in parallel with the original Glan prism. This attenuator returned the intensity to the single-channel circuit i.e., the light reflected by means the electrical resonance after being split by the Glan prism. Such a change lowered the modulation amplitude until the single-channel would function.

APPENDIX B

DETERMINATION OF THE ABSOLUTE RATE OF GAMMA-RAY EMISSION OF THE Hg^{203} STANDARD

A platinum-screen gamma-ray counter, belonging to the Radioactivity Center of the M.I.T. Physics Department, was used for estimating the absolute rate of gamma-ray emission by a sample of Hg^{203}. This sample was eventually used in estimating the efficiency of the scintillation counter for detecting the decay of metastable $^{m}Cd^{111}$. The counter is similar to the platinum-screen counter investigated by Peacock (P2) during his determination of gamma-ray counter efficiencies.

A table of factors has been compiled by the Radioactivity Center for use of the platinum-screen counter with a number of different isotopes. This table makes it possible to determine the absolute number of disintegrations per unit time in a sample of any one of the isotopes by comparison of its counting rate with that of a radium standard when both are located the same distance from the counter. The factors for several of the isotopes with relatively simple gamma-ray decay schemes are plotted against the total energy of the gamma rays emitted in Figure 17. The factor for Hg^{203} was obtained by extrapolating this curve. The Hg^{203} sample and a radium standard were counted for equal periods of time at equal distances from the counter. Runs were made at several distances from the counter to insure that

APPENDIX I

DETERMINATION OF THE ASSOCIATED WATER OF HYDRATED MANGANESE DIOXIDE

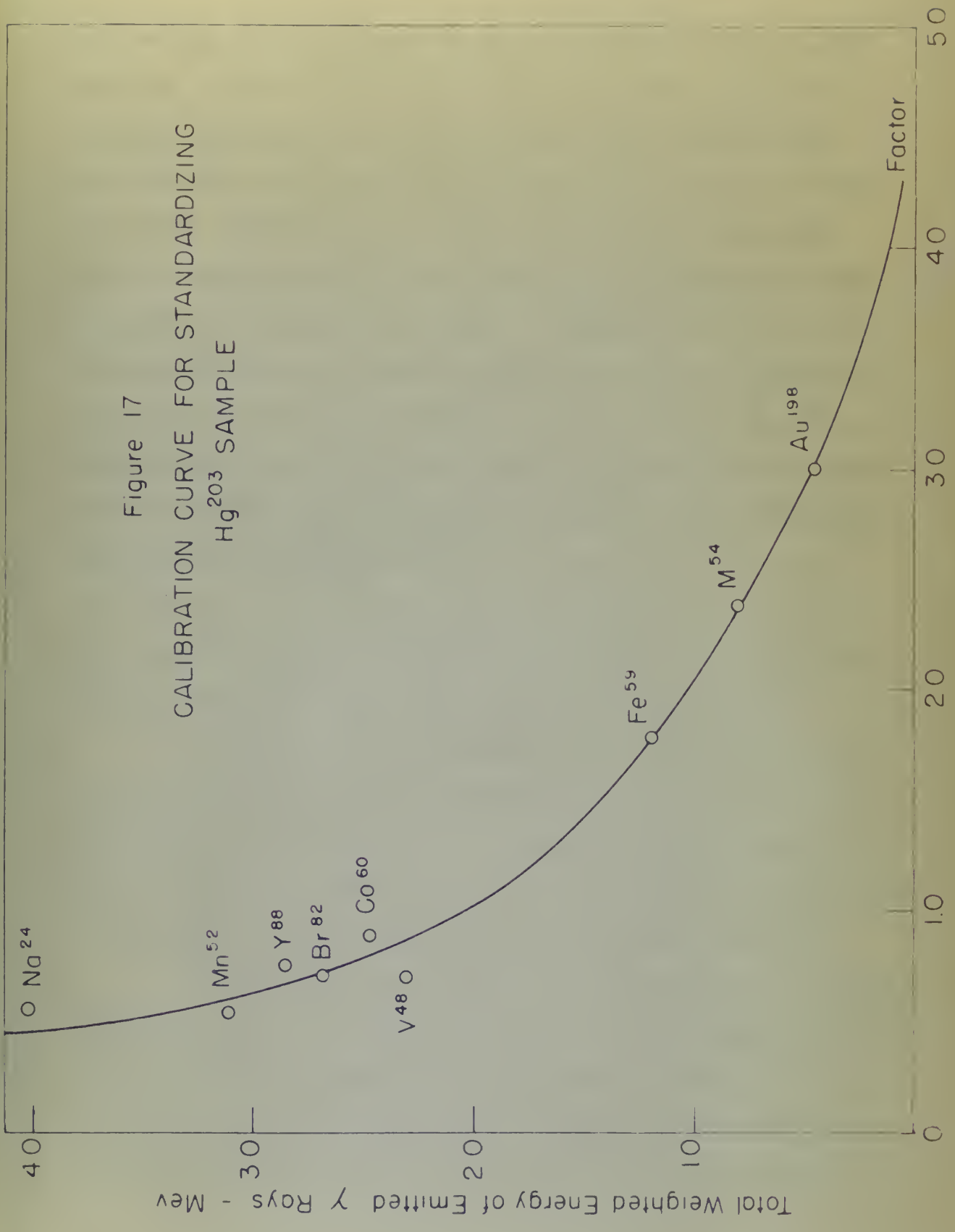
Figure 17
CALIBRATION CURVE FOR STANDARDIZING
Hg^{203} SAMPLE
Total Weighted Energy of Emitted γ Rays - Mev
Factor
0
10
20
30
40
50
Na^{24}
Mn^{52}
Y^{88}
Br^{82}
Co^{60}
V^{48}
Fe^{59}
M^{54}
Au^{198}

the geometry of the sample and the radium standard was approximately the same. The instructions for using the factor are: Compare the net counting rates from the sample and the radium standard at the same distance from the gamma-ray counter. The net counting rate for the sample, multiplied by the factor, is to the net counting rate for the standard as the ratio of their absolute disintegration rates. The extrapolation process is subject to considerable error, and the use of an isotope as a standard for which the factor was definitely known would have been more desirable. However, none of the calibrated isotopes had total gamma-ray energies approximating the single 0.247-Mev gamma ray predicted as comprising 86 per cent of the decay radiation from metastable $^{*}Cd^{111}$.

APPENDIX C

UNSUCCESSFUL PRELIMINARY EXPERIMENTS IN PRODUCING AND DETECTING THE DECAY OF METASTABLE STATES

Samples of Rh^{103} were irradiated with fast neutrons for one hour, but the decay of the 53-minute metastable state was not detected. This isotope is 100 per cent abundant, and from the per cent abundance standpoint, it should be an ideal subject for this type of investigation because no interfering decays will occur. The metastable state decays by the emission of a 0.038-Mev gamma ray. Evidently the cross section for the formation of the metastable state is very small or the counting equipment was not sensitive enough to detect the low energy radiation emitted. Wiedenbeck (W2) reports observing the decay of metastable $^{m}Rh^{103}$ with delicate counters made of rhodium.

Samples of Cb^{93} were irradiated with fast neutrons for one hour, but the decay of the 42-day metastable state was not detected. This failure was probably due to the relatively short time of irradiation. Use of the Rockefeller generator for a period of time comparable to the half-life of the metastable state is obviously impossible.

A sample of mercury deposited on a gold backing was irradiated with fast neutrons for one hour, but decay of the 46.6-minute metastable state in Hg^{201} was not detected. The failure was probably due to a small cross section for the formation of the metastable state and an insufficient abundance of the isotope, Hg^{201}, in natural mercury.

Thesis
F73

Francis

Isomeric metastable states in medium and heavy weight nuclei.